TALLINN UNIVERSITY OF TECHNOLOGY

SCHOOL OF ENGINEERING

Department of Materials and Environmental Technology

STUDY OF THICKNESS EFFECT ON PROPERTIES OF Zn(O,S) LAYERS PREPARED BY PULSED LASER DEPOSITION

PAKSUSE MÕJU UURIMINE IMPULSSLASER-SADESTUS MEETODIL VALMISTATUD Zn(O,S) KIHTIDE OMADUSTELE

MASTER THESIS

Student : Anouar Bouchaara

Student code : 184642KAYM

Supervisor : Assoc. prof. Sergei Bereznev

Co-supervisor : Akram Abdalla Mohammed Ibrahim, PhD student

Tallinn 2020

AUTHOR'S DECLARATION

Hereby I declare, that I have written this thesis independently.

No academic degree has been applied for based on this material. All works, major viewpoints and data of the other authors used in this thesis have been referenced.

"20" May 2020

Author: Anouar Bouchaara

/signature /

Thesis is in accordance with terms and requirements

"20" May 2020

Supervisor: Assoc. prof. Sergei Bereznev.

/signature/

Accepted for defence

".....".....2020

Chairman of theses defence commission: Prof. Malle Krunks

/signature/

TalTech Department of Materials and Environmental Technology

THESIS TASK

Student: Anouar Bouchaara, 184642KAYM

Study programme, KAYM09/18, Materials and Processes for Sustainable Energetics

main speciality: processes for sustainable energetics

Supervisor(s): Assoc. prof. Sergei Bereznev, +372 5560 5390

PhD student Akram Abdalla Mohammed Ibrahim, +372 5351 4990

Thesis topic:

(in English) STUDY OF THICKNESS EFFECT ON PROPERTIES OF Zn(O,S) LAYERS PREPARED BY PULSED LASER DEPOSITION

(in Estonian) PAKSUSE MÕJU UURIMINE IMPULSSLASER-SADESTUS MEETODIL VALMISTATUD Zn(O,S) KIHTIDE OMADUSTELE

Thesis main objectives:

1. Deposition of Zn(O,S) layers with different thicknesses on SLG substrates at 300°C using pulsed laser deposition method.
2. Structural, morphological, optical and electrical characterization of the obtained Zn(O,S) structures.
3. Analysis of obtained results, formulations of discussion and conclusions.

Thesis tasks and time schedule:

No	Task description	Deadline
1.	Literature overview, setting the aim of the study	31.11.2019
2.	Experimental work, evaluation of results	29.02.2020
3.	Writing of the thesis	16.05.2020

Language: English **Deadline for submission of thesis:** "26" May 2020

Student: Anouar Bouchaara ..... "....."..... 2020

/signature/

Supervisor: Sergei Bereznev ..... "....."..... 2020

/signature/

Co-supervisor: Akram Abdalla Mohammed Ibrahim ..... "....."..... 2020

/signature/

Head of study programme: Sergei Bereznev ....."....."..... 2020

/signature/

Contents

PREFACE

The present topic of study was introduced by supervisor Dr. Sergei Bereznev, with co-supervisor Akram Abdalla Mohammed Ibrahim, PhD student (Taltech). The major thesis research was carried out at the Laboratory of Optoelectronic Materials Physics, Department of Material and Environmental Technology, Tallinn University of Technology.

I would like to express my special thanks and appreciation to my supervisor, Dr. Sergei Bereznev, for his support, patience and valuable expertise shared on my way to graduation. I would also like to express my sincere thanks to my co-supervisor, Akram Abdalla Mohammed Ibrahim, for helping me to carry out this research and to learn a lot of new scientific information about the laboratory and the project. I would also like to thank Dr. Valdek Mikli and Dr. Erki Kärber for their help in sample characterization, and for their support and consultation in collecting data. I would also like to thank Prof. Malle Krunks for her guidance and shared knowledge during my study time. I am grateful as well for the support of my family and friends. This work was supported by project TK141 of the European Regional Development Fund.

In previous reports, several authors reported Zn(O,S) as one of the emerging Cd-free buffer layers with properties close to CdS thin films. The effect of the deposition parameters on the Zn(O,S) layers has also been reported. However, the impact of film thickness on the characteristics of the Zn(O,S) layer has not yet been thoroughly studied.

The aim of this work is therefore to deposit Zn(O,S) buffer layers using the pulsed laser deposition (PLD) technique and investigate the thickness effect on its properties.

Firstly, a literature analysis of the functional layer, buffer layer comparison, Zn(O,S) buffer layer properties and various deposition techniques used for Zn(O,S) thin film are discussed in different sections. Secondly, the PLD technique was used to deposit samples of various thicknesses. All prepared samples were characterized using instrumental methods of analysis. Finally, the discussion of the results of characterization of the thickness effect on properties of Zn(O,S) layers formed by pulsed laser deposition was performed. The results suggest that variations in film thickness have a small effect, in particular, on optical and electrical properties of obtained layers.

Keywords: Zn(O,S), buffer layer, thickness effect, pulsed laser deposition, master thesis.

LIST OF ABBREVIATIONS

ALD	Atomic laser deposition
AFM	Atomic force microscopy
AZO	Aluminum doped zinc oxide
CBD	Chemical bath deposition
CIGS	Copper Indium Gallium Sulfide
CIGSe	Copper Indium Gallium Selenide
CZTS	Copper Zinc Tin Sulfide
DC	Direct current
EDX	Energy dispersive X-ray spectroscopy
FF	Fill factor
FTO	Fluorine doped tin oxide
HR-SEM	High resolution scanning electron microscopy
ITO	Indium tin oxide
JCPDS	Joint Committee on Powder Diffraction Standards
J_{sc}	Current in short circuit
PLD	Pulsed laser deposition
PV	Photovoltaic
RF	Radio frequency
RT	Room temperature
SC	Solar cell
SLG	Soda lime glass
TEM	Transmission electron microscopy
TFSC	Thin film solar cell
UV	Ultraviolet
V_{OC}	Voltage in open circuit
XRD	X-ray diffraction

INTRODUCTION

Power conservation plays a vital role in ensuring the creation of a prosperous environment and greater quality of life. Seeing that the fossil fuel supplies are expected to run out, the planet desperately needs to find new environmentally sustainable energy sources. The greenhouse gas emissions increased as CO_2 emissions in 2019 reached 33 GT of CO_2 [1] due to excess fossil fuel consumption. Countries, organizations, and regions adopt the idea of renewable energy each coming year in order to meet the 7th Renewable Development Goals (SDG) target. The planet is turning to renewable energy sources as the existing energy supply is non-renewable and the global market for power, heating, cooling and transportation is getting more disruptive [2,3]. Consequently, solar energy is considered one of the most important options for meeting earth's demand for zero-emission energy [3].

The amount of energy the Planet receives from the sun is considerably large and is projected as a source of renewable energy to sustain all aspects of life on Earth. The planet receives approximately 1.7×10^{11} MW of solar energy annually [4], which is only 0.1 per cent of the total energy capacity of the sun. Furthermore, 1h of the solar energy received by the earth is equal to the annual global energy consumption [4].

Solar cells are one approach to harvest the sunlight energy and produce electricity. They can be prepared on the basis of semiconductor materials with suitable optoelectronic properties [5]. The search for higher solar cell efficiencies has been ongoing in recent decades since the discovery of the photovoltaic effect [5].

At the moment, silicon solar cells are the most common on the market with a conversion efficiency of roughly 21.2 to 26.7% [6]. While silicon is one of the most abundant elements on earth, purification and photovoltaic processing using silicon as a material was previously one of the greatest challenges as it was an energy demanding process. As a result, the development of the ultra-thin amorphous layers of silicone of the second generation was initiated as an alternative. Solar cells with silicon thin film may typically be deposited on glass or plastic by vaporization or chemical methods. Such cells have the working characteristics under low intensity light conditions which are a great advantage [7,18]. New absorbers have also been developed for thin-film solar cells, such as CuInGaSSe (CIGSSe), CdTe, GaAs and CuZnSnSSe (CZTSSe) thin films, which can produce device efficiency

higher than 20% [6]. On the other hand, the quality, cost of processing and toxicity of some of them remain a challenge [6,8,9].

N-type semiconductor, which is commonly known as a buffer layer, is required to form a p-n junction in complete solar cell structure. These buffer layers should be almost transparent for sunlight. In the last decades, CdS films were commonly used as buffer layer with different absorbers and achieved high efficiencies up to 22.9% [6]. However, CdS have been reported as a toxic material and absorbs a part of the light due to its relatively narrow band gap of 2.45 eV [9]. Thus, there is a trend of replacing the CdS layer with less-toxic materials and wider band gap. Among them, the Zn(O,S) is one of the promising materials that has shown its applicability to function as a buffer layer in thin film solar cells [10]. Due to its wide band gap in the range of 2.8–3.7 eV [11,12], the Zn(O,S) thin films can be considered as a possible alternative to the CdS buffer. Another advantage of Zn(O,S) is that Zn, O and S are earth abundant and eco-friendly elements [13]. Zn(O,S) films can be produced using various methods such as chemical bath deposition (CBD) [11], sputtering [15], atomic layer deposition (ALD) [16] pulsed laser deposition (PLD) [17], etc. The PLD method has several advantages mentioned in earlier reports, one of the key advantages of which would be the stoichiometric deposition of the target material, which allows the production of thin films with less waste of the initial component [18].

The optoelectronic properties of Zn(O,S) thin film deposited by PLD in high-vacuum were investigated in this research. The effect of thickness dependence was studied in order to analyze the correlation between the structural, optical and electrical properties of the obtained layers with increasing the thickness of the film. The current thesis is structured as follows:

1. Chapter 1 introduces the functional layers in solar cells, compares different Cd-free buffer layer, the properties of Zn(O,S) films and the impact of deposition conditions, the deposition methods and the effect of thickness dependence for Zn(O,S) films.
2. Chapter 2 describes the apparatus and methodology for the experimental part and the techniques of characterization used for film deposits.
3. Chapter 3 discusses the results that have been reached.
4. Chapter 4 presents conclusions from the findings gathered.

1. LITERATURE OVERVIEW

1.1 Functional layers in solar cells

Thin film solar cells (TFSCs) devices are composed usually of several layers called "functional layers" [19,20]. Each layer can be different in terms of crystal structure, chemical composition, diffusion coefficient, mechanical and electrical properties, etc. [19]. Usually, the thin film solar cells contain the following layers (Figure 1.1):

- Front and back contact layers
- Absorber layer (p-type)
- Buffer layer (n-type)

The back contact consists usually a metal film with ohmic contact properties [20]. On the other hand, the front contact is anti-reflective and highly transparent in the visible range. In most cases, this layer contains a transparent conductive oxide (TCO) such as FTO, ITO or AZO [19]. Both the front and back contact must be highly conductive [20].

The (p-type) absorber layer is a crucial layer in the solar cell device and it should have high absorption coefficient, high mobility of charge carriers and low recombination rates with a relatively narrow band gap in the range of 1.1 to 2.0 eV [19-22], where the absorption of light take place. Different materials were investigated and applied as an absorber in thin films solar cells such as amorphous silicon (a-Si), Copper Zinc Tin Sulfide (CZTS), Copper Indium Gallium sulfide/Selenide (CIGSSe), Gallium arsenide (GaAs), Cadmium Telluride (CdTe), some photosensitive organic semiconductors (dyes, pigments and polymers), etc. [19,24,25].

The buffer layer is usually an n-type thin film combined with a p-type absorber layer to form the p-n junction. Buffer materials have a higher band gap values in comparison with photoabsorbers (in the range of 2.4-3.6 eV) (mainly transparent in visible range of spectrum). As a rule, thickness of buffer layer is lower than thickness of photoabsorber layer (between 20 and 500 nm) in order to decrease series resistance losses and waste of material [20,22]. Figure 1.1 shows a schematic drawing of conventional thin-film solar cell (TFSCs) in superstrate and substrate configurations.

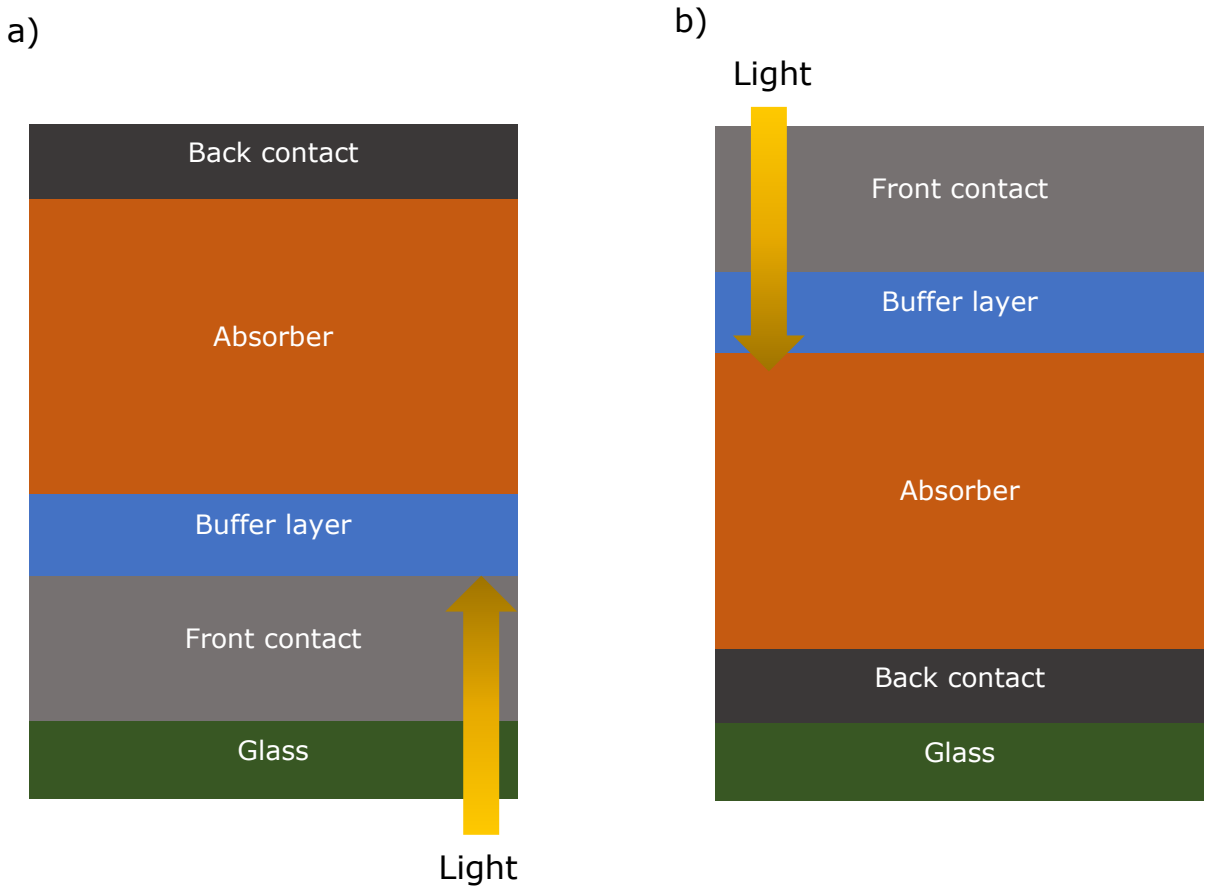

Figure 1.1: Schematic drawing of TFSCs configuration: (a) superstrate structure (b) substrate structure.

Although, CdS as a buffer demonstrates excellent device performance, its toxic material and has a parasitic absorption at 350 – 500 nm. As a result, currently there is investigations focused to find an alternative non-toxic and wider band gap materials [26]. According to Hariskos et al. [27], several buffer layers are promising to replace CdS buffer layers and with similar efficiencies which will be discussed in the following part 1.2 with more details.

1.2 Comparison of different Cd-Free buffer layers

In the past decade, a number of laboratories used CdS as a buffer layers produced by chemical bath deposition (CBD) to be combined with such absorbers as CIGS,

CdTe, CZTSSe, etc. Up-to-date, CBD technique is preferred by the manufacturers over vacuum deposition to produce CdS buffers as it offers uniform coverage of the absorber surface with high interface quality, and already reached higher device performance [28]. In recent studies, a record of conversion efficiency was achieved on laboratory scale which was about 22.92% for ZnO/CdS/CIGSSe thin film configuration device [29]. However, concerns were raised for the use of CdS buffers, which are as follows:

- Environmental impact factor indicates the use of CdS involves risks of toxicity for the eco-system [30,31]
- Parasitic absorbance which interfere with conversion efficiency of the TFSCs devices [32]
- European regulations (Directive 2002/96/EC [33]) have decided to prevent the use of cadmium in electronic devices.

In the research reported by previous articles [6,34], the technology process for producing thin film solar cell has been focusing recently to achieve Cd-free buffer layers. New materials are in sight to be used as eco-friendly with a higher band gap. According to [28], Zinc-based, Indium-based and other emerging buffer layers have been frequently studied as Cd-free layer, considered as a promising alternative for CdS layers. The deposition technique and materials used for these new buffer layers is important to reach efficiencies closer or superior than for the CdS buffers level [34]. Table 1.1 shows an example of Zn-based and In-based buffer layers obtained by different deposition methods used for each one. It shows also different PV parameters as a result of the research done previously on complete configuration including these buffers.

Table 1.1 : summary of the Cd-free buffers used in solar modules

Buffer layer	Absorber	V_{oc} V	J_{sc} mA/cm^2	FF %	η %	Ref
Zn(O,S)	$Cu(In,Ga)Se_2$	0.72	37.2	78.6	21.0	[35]
	CdTe	0.59	21.0	64.2	8.0	[36]
	Cu_2ZnSnS_4	0.48	17.2	55.5	4.6	[37]
Zn(O,OH,S)/(Zn,Mg)O	$Cu(In,Ga)(S,Se)_2$	0.73	39.6	80.4	23.35	[38]
Zn(O,OH,S)	$Cu(InGa)Se_2$	0.66	37.7	75.7	18.8	[39]
In_2S_3	$Cu(In,Ga)(S,Se)_2$	0.63	35.5	72.0	16.1	[40]
$Zn_{1-x}Sn_xO$	$Cu(In,Ga)Se_2$	0.69	35.1	75.3	18.2	[41]
	Cu_2ZnSnS_4	0.68	21.6	61.4	9.3	[42]

According to Table 1.1, Zn(O,S) layers is one of the most promising Cd-free buffer layers that are currently under investigation and development with results comparable to the other Cd-free material type buffers.

1.3 Zn(O,S) buffer layer

In the last decades, several studies have been focused to investigate Zn(O,S) as a buffer layer material for thin film solar cell devices (TFSCs). It has been reported that Zn(O,S) layer is an n-type semiconductor having attractive characteristics such as non-toxic, contain earth abundant elements, good electrical and optical properties with the band gap around 2.8-3.75 eV [43-46]. In addition, recycling issues could be reduced during the deposition of Zn(O,S) buffers [47,54]. However, the quality of Zn(O,S) films could be affected by deposition conditions.

The elemental composition of Zn(O,S) layers can affect the electrical properties of complete solar cell structures that studied e.g. in a CZTS solar cell configuration. Ericson et al [48] have studied the influence of the variation of oxygen to sulfur ratios in Zn(O,S) films on the performance of the Cu_2ZnSnS_4 (CZTS) solar cells structure. The deposition was achieved via atomic layer deposition of pure ZnS, pure ZnO and Zn(O,S) layers by variation of film composition to obtain different oxygen to sulfur ratios (from 4:1 to 9:1). It was observed that pure ZnO layers demonstrate a low open circuit voltage (V_{oc}) value while pure ZnS film demonstrates a current blocking properties. This comes in agreement with the description of Barkhouse et al [46] for the electrical properties of ZnS and ZnO films. On the other hand, Ericson et al [48] reported that the highest values of V_{oc} and the current in short circuit (J_{sc}) were obtained for the Zn(O,S) film with a higher amount of sulfur concentration. Although the fill factor (FF) was higher for samples with intermediate ratios, it was observed that with the increase of sulfur content, there is an increase of the activation energy for recombination [48].

Another study of the effect related to oxygen and sulfur ratios for Zn(O,S) layers on their optoelectronic properties was performed by Hong et al [49] using the atomic layer deposition method (ALD). It was shown that the optical band gap of the ALD Zn(O,S) films is highly dependent on the growth cycle ratio (GCR) [49]. In which according to the experiment made, the GCR increases for ALD Zn(O,S) samples with high oxygen content, while it decreases for ALD Zn(O,S) samples with a high amount of sulfur. The band gap value observed is in the range of 2.8-3.6 eV. Low resistivity has been observed for the Zn(O,S) films with a temperature above 170°C. Woo-Jin Choi et al [50] have confirmed that the improved S/(S+O) ratio of 0.20 (4:1 oxygen

to sulfur ratio) in Zn(O,S) layers achieved an efficiency up to 17.1% in the laboratory scale with CIGS TFSCs structure.

Another type of solar cell device such as SnS photoabsorber based TFSCs structure studied by Sinsermsuksakul et al [51] has reached a power-conversion efficiency of 2.46% following an optimal S/Zn ratio in the range of 0.37-0.50. The following configuration of solar cell device (SLG/Mo/SnS/Zn(O,S)/ZnO/ITO) was used to study the performance of the SnS TFSC. The Zn(O,S) films were deposited by ALD method at 120°C in a vacuum atmosphere while varying the cycle of ZnO to ZnS ratios (from 4:1 to 7:1) during the deposition process. It was observed that Zn(O,S) samples demonstrate a positive value (spike) of conduction-band offset (CBO) at the interface of SnS/Zn(O,S) layers with the increase of sulfur content.

Recent studies show that not only the variation of oxygen to sulfur ratio has an effect on Zn(O,S) buffer layers, but also deposition temperature has influence. Bugot et al [52] prepared Zn(O,S) films by atomic layer deposition process and investigated the temperature effect on their optoelectronic parameters. The ALD deposition of Zn(O,S) layer was carried out with a 210 repeated cycle that includes diethylzinc ($Zn(C_2H_5)_2$), hydrogen sulfide and deionized water. Nitrogen was used as purging gas; deposition temperature was varied from 120 to 260°C with an oxygen to sulfur ratio of 0.14. The ALD Zn(O,S) films were deposited on CIGS layers to study the solar cell performance [52]. It was observed that increase of fill factor and efficiency (up to 13.8% for CIGS solar cell) with the increase of temperature up 220°C. However, the variation of temperature from 140-160°C shows overall good CIGS cell performance. This was explained by the favorable optoelectronic properties of ALD Zn(O,S) film deposited in the temperature range of 140-180°C [52]. In a previous study done by the same group [53], it was shown that ALD Zn(O,S) films formed at 140-160°C have better conductivity, high carrier concentration and an optical bandgap of ~3.16 eV. Additionally, Bugot et al [52] concluded that the rise of sulfur content is related to the rise of deposition temperature above 180°C. However, for lower temperature, the composition remained unchanged. For temperature between 160 to 180°C, a decrease in the band gap and resistivity occurred.

Another recent investigation done by Khemiri et al [54] regarding the optoelectronic properties of Zn(O,S) thin films using sputtering deposition method. the deposition temperature was prominent, which was used as Cd-free buffer layer in TFSCs. It

was found with the increase of deposition temperature of sputtered Zn(O,S) films, the sulfur content increased. The high crystallinity of these Zn(O,S) films reduces the volume of defects and grain boundaries. Thus, leading to a minimum of absorption and light scattering.

Another study was performed by Jani et al [55] in which they demonstrate that the annealing atmosphere influence on Zn(O,S) films optoelectronic properties. The Zn(O,S) were deposited by spray pyrolysis deposition where a solution contained zinc chloride ($ZnCl_2$) and thiourea (CH_4N_2S) precursors dissolved in isopropyl alcohol and deionized water. Thiourea was employed as Sulphur source for Zn(O,S). Annealing treatment was used after deposition of Zn(O,S) layers at 370°C in air and argon atmosphere for 1h [55]. All samples were observed to have a hexagonal crystal structure with an orientation of (100), (002), (101) planes according to JCPDS 36-1451 [55]. The optical band gap values were found to be between 3.3 to 3.6 eV. However, It was stated by authors [55] that the uniformity of Zn(O,S) films is influenced by the change of annealing atmosphere. The grain boundaries are less prominent in air annealing atmosphere rather than annealing in argon atmosphere according to AFM analysis. According to Jani et al [55], annealing treatment helps decreasing the defect density and increase the conductivity by reducing the capture of charge carrier. The annealing treatment in air allows to increase the amount of carrier concentration up to 10^{15} cm^{-3} for the Zn(O,S) films obtained. However, the conductivity of Zn(O,S) films was observed to be improved more by annealing in argon atmosphere.

In conclusion, several reports [43-55] attest on the optoelectronic properties of Zn(O,S) buffer layers. Still, the oxygen to sulfur ratio, deposition temperature and annealing atmosphere [48-55] can influence the characteristic of the Zn(O,S) films and solar cell performance. Furthermore, the choice of deposition method also affects the properties of these buffer layers, which will be discussed in the following section.

1.4 Deposition techniques for Zn(O,S) thin films

The Zn(O,S) buffer layers can be applied as an alternative for the CdS buffer layer. In these reports, several thin film deposition processes have been described e.g. chemical bath deposition [56-66], spray pyrolysis [67-73], atomic layer deposition [74-81], sputtering [82-91], pulsed laser deposition [92-101] and other deposition methods [102-104]. The choice of the deposition method affects differently on the properties of resulted Zn(O,S) films.

1.4.1 Chemical bath deposition

Chemical bath deposition (CBD) technique or solution growth method to make thin films layers through a continuous chemical sedimentation. The substrates are submerged into a dilute chemical solution containing the target precursors. The process involves particle growth through nucleation, which leads to the formation of a solid phase from a solution [56]. Figure 1.2 shows the schematic illustration of the chemical bath deposition method. CBD was commonly applied for the deposition of CdS buffers to obtain high efficiencies and pinhole-free surface layer [56,57].

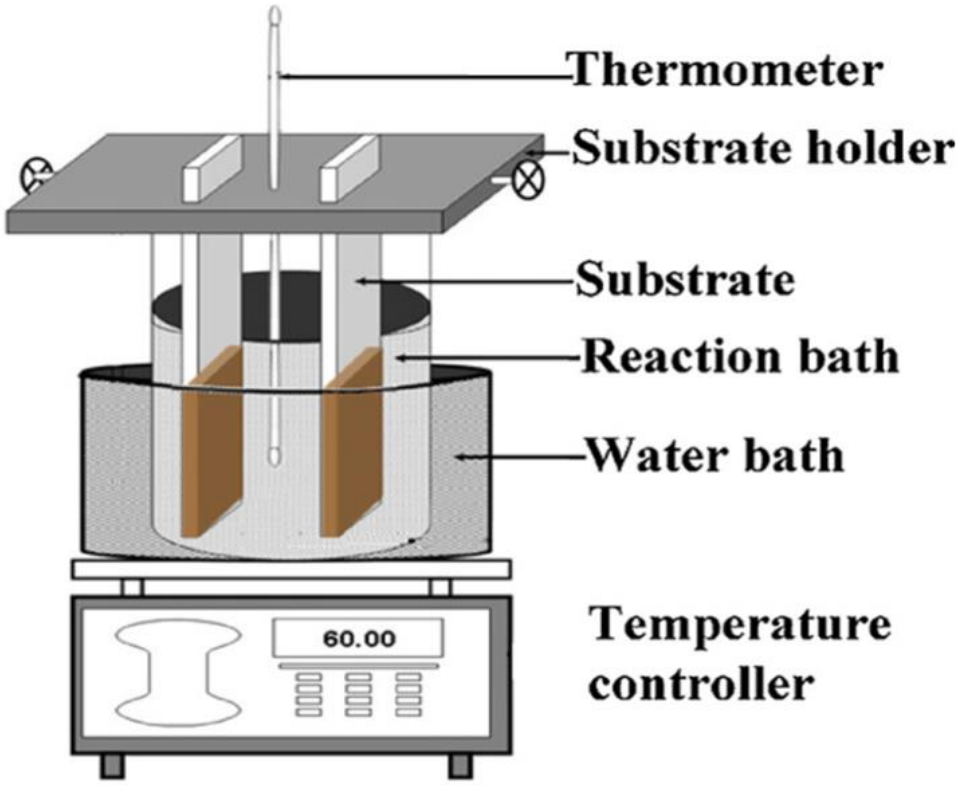

Figure 1.2: schematic illustration of the chemical bath deposition setup [60]

This method is well-known for the following advantages:

- Low-cost method as the precursor materials are widely available and inexpensive [57,66].
- Relatively simple since it does not require costly and advanced equipment to perform the deposition [56,57].
- Possibility of multiple deposition on several substrates could be carried out at the same time for the same material [57,61]. Therefore, the CBD is suitable for large scale industrial manufacturing.
- Large area of deposition and the deposition parameters are controlled easily [57].

In contrast, the CBD method has also some disadvantages, such as:

- The wastage of chemical solution can occur after deposition [58].
- Slow deposition rate for producing thick layers and there is a probability of peeling that can happen after deposition [58].
- The formation of large size particles (aggregates) and impurities inside the thin film can occur due to precipitation. This could affect the optical and electrical properties of deposited films [57,58].
- Appearance of undesired hydroxides or oxides compounds within the formed thin films using CBD was reported in previous articles [66]. Thus, contamination is another disadvantage of chemical bath deposition method.

Among the recent research made, Buffière et al [64] tried to optimize the deposition time of CBD grown Zn(O,S) layers according to what was described in earlier reports. The use of H_2O_2 in the bath aqueous solution leads to the increase of the oxygen amount, making the reaction time faster. The obtained Zn(O,S) layers using H_2O_2 as secondary precursor were compared with deposited CBD-Zn(O,S) samples prepared by the standard method mentioned in previous articles [65]. The authors [64] observed that the deposition time of the films using H_2O_2 precursor was 5 min faster than the as-deposited conventional CBD-Zn(O,S) layers. The optical band gap was around 3.85 eV for the layers prepared by the conventional CBD process, which was slightly wider than for the Zn(O,S) samples with band gap value of 3.75 eV produced by the fast-deposition method [64]. It was reported that both zinc oxysulfide films have similar efficiencies with a CIGSe solar cell structure. Fast-deposited Zn(O,S) have demonstrated 12.2% efficiency while the standard-

deposited showed 11.6% with a CIGSe Solar cell. Lastly, M. Buffière et al [64] suggested the use of this fast-growing CBD method rather than the conventional CBD procedure used previously in manufacturing and research studies.

Gautron et al [65] also studied the properties of Zn(O,S) buffers following their deposition by CBD method and their performance with a CIGSe solar cell device. The Zn(O,S) layers were deposited on co-evaporated CIGSe absorber layers at 70°C in a solution bath containing zinc sulfate heptahydrate, ammonia and thiourea as precursors[65]. After the deposition of Zn(O,S) films, the samples were immersed in a NH_3 solution to avoid any precipitated particles in the film structure. The S/(S+O) ratio was found to be 0.60 for all deposited Zn(O,S) films with good coverage and thickness of 20 nm[65]. However, the morphology and structural analysis revealed the presence of two distinct layers inside the Zn(O,S) layer. According to the authors [58], the first layer of the Zn(O,S) films exhibited a ZnS phase oriented towards (111) plane and parallel to the (112) plane characterized for CIGSe chalcopyrite layer. For the second layer, it was observed the presence of a mixture ZnS and $Zn(OH)_2$ phases [65]. However, the efficiency of CBD grown Zn(O,S) films was higher compared to the literature described in the article. This is due to an improved carrier conductivity in the Zn(O,S) structure. Gautron et al [65] demonstrated that the CIGSe TFSC characteristics with Zn(O,S) buffer using CBD depend strongly on their microstructure.

To sum-up, chemical bath deposition has attracted the attention of many researchers and manufacturers in the last decades. Several advantages and drawbacks have been observed [56-66]. The authors [64,65] report a uniform and good surface coverage of the deposited films using CBD. However, there is an influence of deposition conditions on the structural and electrical properties of Zn(O,S) films using this method [64].

1.4.2 Spray pyrolysis

It is an aerosols process that includes an atomizer, precursor solution, a substrate heater, and a temperature controller. The first step of this deposition technique

begins with the atomization of the liquid solution into fine droplets which are sprayed afterward on the substrate [67,68,71]. The type of atomizer used can be "air blast" which exposes the liquid to an air stream, ultrasonic frequencies to produce short wavelengths in order to obtain adequate atomization or using a high electric field. Then comes the decomposition of the droplets at high temperatures with the help of a hot plate to make solid particles forming the surface of the layer [67,71]. Figure 1.3 demonstrates the schematic of spray pyrolysis working principle.

The simplicity of the process is among the main advantages of the spray pyrolysis method since it doesn't require advanced and expensive equipment for the deposition of thin films [67,69]. Thus, spray pyrolysis is a low-cost deposition method that allows obtaining dense thin films. According to Alves et al [67], it can be applied to large deposition area which is suitable for large-scale production of TFSCs. In addition, the control of film composition can be easily achieved through the precursor solution [68,69]. Spray pyrolysis has a wide range of applications besides solar cell fabrication (e.g. for sensors) [67].

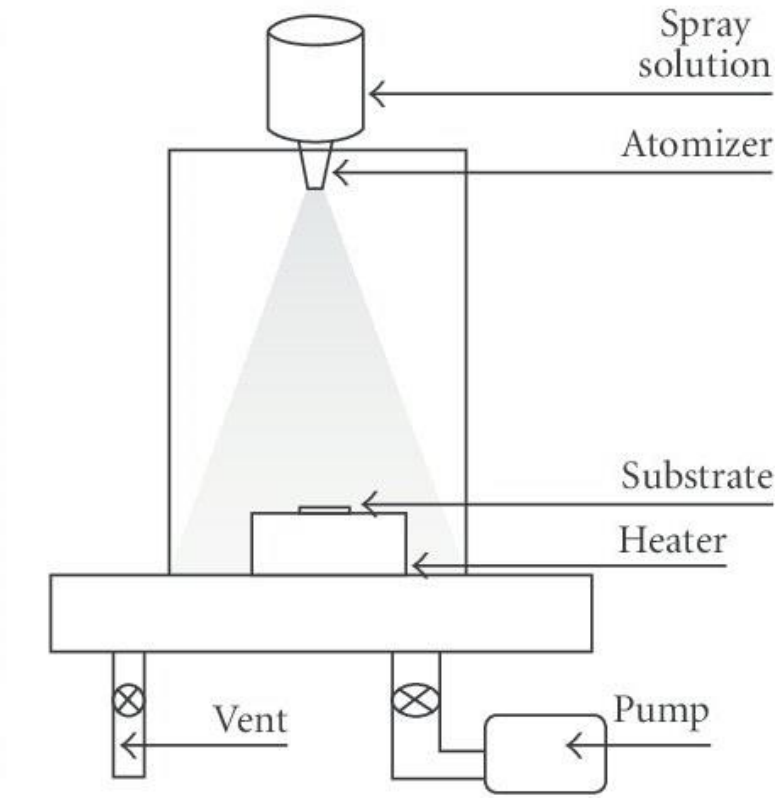

Figure 1.3: schematic illustration of spray pyrolysis deposition process [73].

However, it has been stated that spray pyrolysis has some drawbacks which are known to be related mainly to the formation of droplets during the deposition of thin films [67]. This leads to produce defects such as non-uniformity, porosity or cracks inside the thin layers [70]. Furthermore, the risk of contamination can occur during the deposition of the layers [67,70]. Similarly, to the CBD method, spray pyrolysis has a slow deposition rate and wastage of chemical material [70,71].

In the paper of Polat et al [72], an investigation of Zn(O,S) buffers was done using spray pyrolysis deposition on a glass substrate. The aim of this research was to compare the optoelectronic properties of Ni-doped and non-doped zinc oxysulfide samples deposited and annealed under vacuum. The deposition was performed using a solution of zinc chloride ($ZnCl_2$) and thiourea [$SC(NH_2)_2$] mixed with deionized water [72]. The spray rate of the solution on the substrate was approximately 2 ml/min with air as a carrier gas. The heating temperature was 490°C during the process. Electron beam evaporation was used for doping Zn(O,S) layers with Nickel element and compared with as-deposited Zn(O,S) to study the diffusion effect [72]. The annealing process was performed at various temperatures in a vacuum of 2×10^{-5} Torr. Polat et al [72] observed that the obtained films have a uniform thickness between 2.5-3.5 µm. After characterization, both films show low average transmittance between 8 to 35% in the wavelength range of 190 to 1100 nm. The band gap was found to be 3.38 eV for as-deposited films and 3.44 eV for doped films [72]. The XRD results showed that the as-deposited Zn(O,S) films have a Wurtzite structure oriented (002) with a mixture of ZnS and ZnO phases. Whereas, doped Zn(O,S) showed a hexagonal crystal structure oriented (002) in addition to (110),(103) planes. Polat et al [72] suggested that substitution of zinc elements occurred with Ni ions within doped Zn(O,S) films, this led to an improvement of crystallinity for doped Zn(O,S) layer structure.

In summary, spray pyrolysis is a chemical deposition method which is widely used for the main advantage mentioned in this section [67-69]. However, this technique has also several disadvantages that can leads to the presence of defects [67,70,71]. Additionally, the authors [71] stated the influence of deposition parameters using spray pyrolysis on the optoelectronic Zn(O,S) buffer layers.

1.4.3 Atomic layer deposition

The principle of the atomic layer deposition (ALD) process is the use of a growth surface mechanism by a repeated sequence of reactions including two different precursors. The formation of a thin film is achieved as a result of one of the reactant's monolayer enters a recurring reaction called "deposition cycles" with the second reactant. This occurs with the help of an intermediate reactor with the help of a purging gas as shown in figure 1.4 [74,75]. Then the surface is subjected to heat treatment making a uniform polycrystalline or amorphous thin film. This technique was first reported by Suntola's work in the 1970s used for growing a distinctive polycrystalline dielectric thin film [76]. The ALD was applied for producing semiconductors thin film such as silicon and GaAs [74].

The advantage of ALD is connected with high controllability of this method accompanied with high atomic precision during the pulsing process. It ensures the thickness uniformity of the surface due to the self-limiting reactions that happen during the procedure [74]. This precise control is mainly because of the partial monolayer growth for each cycle deposition allows a sub-nanometer control over the layer's surface. The reactor purging role is to avert the formation of defects inside the layer [77].

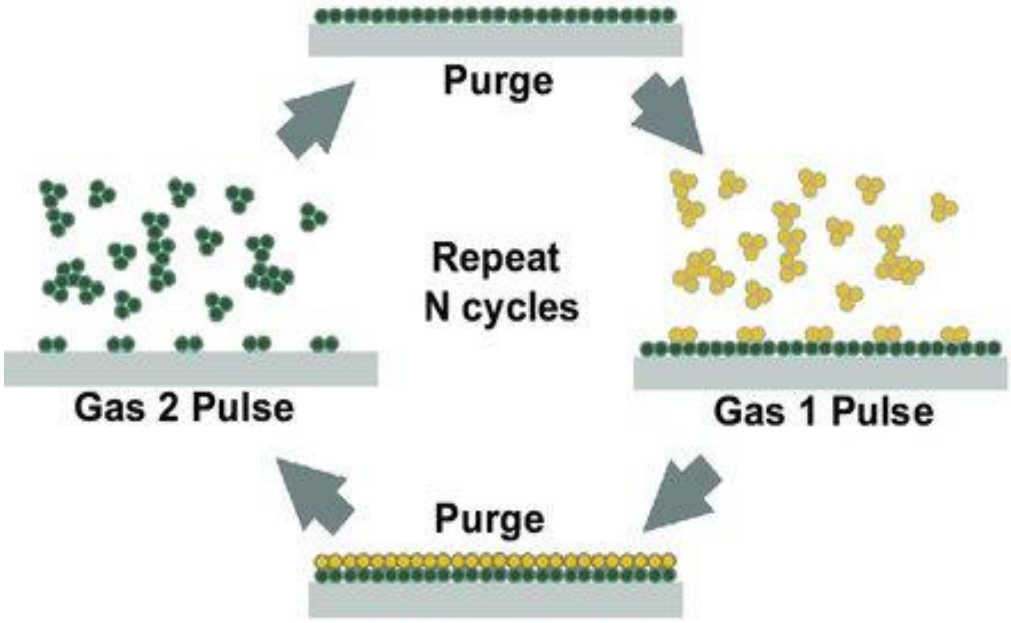

Figure 1.4: schematic illustration of the atomic layer deposition process [78].

Although the use of the ALD technique has several advantages, it has some downsides as well according to Larsson et al [79] such as the choice of precursors and start reaction materials that could affect the fill factor and decrease the efficiency as a result of poor etching and annealing. The heat treatment also could affect electrical characteristics. However, the main limitation of the ALD method is related to the cost of suitable precursors, reactant and gas materials used to deposit the ALD layers. Therefore, this leads to an increase in the operational cost for a higher purity level of thin film deposition and to avoid risks of contamination for ALD grown films [77]. Additionally, the ALD process requires a low deposition rate with many deposition cycles before obtaining the desired functional thin film [74,77].

Several reports mention the use of ALD to deposit Zn(O,S) buffer layers and investigate their characteristics. Lin et al [80] deposited Zn(O,S) buffer layers using ALD method and attempted to combine it with CIGS absorber as a solar cell structure. The samples were grown in a reaction solution for 120 min including zinc sulfate ($ZnSO_4$) and thiourea ($(SC(NH_2)_2$). ALD Zn(O,S) film thickness was in the range from 26.71 to 196.80 nm. It was found, that the Zn(O,S) film with a thickness of 106.84 nm exhibited a transmittance higher than 90% in the visible wavelength range. The optical band gap of All the ALD Zn(O,S) films was observed to be around 3.61 to 3.65 eV[80]. According to this report, An optimized thickness leads to an improved photoconversion efficiency, which was about 11.65% for CIGS solar cell device with a thickness of 106.84 nm for ALD Zn(O,S) buffer layer. It was stated [80] that the examined CIGS solar cell device structure was found to enhance the rate of recombination at the interface of the Zn(O,S) buffer layer and the CIGS absorber layer.

Platzer-Björkman et al [81] prepared Zn(O,S) buffer layers using atomic layer deposition and investigated their performance in a CIGS solar cell. The layers were deposited at 120°C by an alternation of sequence cycle including diethylzinc (DEZ), H_2S and H_2O. N_2 was used as a purging gas and pulse duration was varied from 200 to 400 ms in 500 cycles on SLG. The S/Zn ratio was found to be increasing from 0.1 to 0.9 with the increase of sulfur concentration in Zn(O,S). The authors [81] explain that the increase of sulfur content by the occurrence of reaction between precursors and deposited elements in each pulse. The structure was found to be amorphous for Zn(O,S) with S/Zn ratio between 0.3 to 0.5 and crystalline for the other samples with a mixture of ZnO and ZnS phases. The optical band gap was found to be in the

range of 2.6-3.1 eV [81]. The resistivity of the films was observed to increase with the rise of sulfur concentration. An efficiency up to 16.4% was attained for CIGS solar cell device for Zn(O,S) buffer layers with an S/Zn ratio of 0.3,0.8,0.9 respectively.

To put it concisely, several reports [74-79] mention the use of ALD to deposit Zn(O,S) layer. The properties of the Zn(O,S) layers changed depending on the cycle duration, deposition temperature and material used among other factors mentioned above. Efficiencies were reported [80,81] to vary from 11.65 to 16.4% with different solar cell devices.

1.4.4 Sputtering

The sputtering deposition technique is known as one of the physical vapor deposition (PVD) method commonly used for thin-film manufacturing among other applications such as semiconductor production, surface treatment and jewelry fabrication [82]. The process of sputtering is based on the ejection of atoms from the target surface by collision with an incident energized ion particle. The incident ion particle is by the means of an electrical potential filed created by an anode and cathode which generates an acceleration of ionized atoms in a vacuum chamber [82,83]. The ejected atoms form with energetic ion particles what is called a "plasma discharge" directed from the cathode side towards the anode side where the substrates is located as shown in figure 1.5. The condensation of the ejected atoms on the substrate surface form then a thin film layer through the nucleation process. The accelerated ionized atoms are from a neutral gas composed of inert atoms such as argon (Ar) to avoid any chemical reaction with the target material. Inert gases such as argon are commonly used for the reason that the atomic mass is similar to many metals used in the fabrication process of the thin films [83-85].

The most widely used types of sputtering process are introduced briefly:

- DC sputtering: based applying an electric field for ion acceleration with the help of a DC diode (direct current diode) and two plates (cathode and anode) in a vacuum chamber after introducing the sputtering inert gas [83].

- RF sputtering deposition: radio frequency (RF) sputtering uses high frequency voltage above 1 MHz to maintain a constant plasma discharge composed from neutral and charged particles for a longer sputtering process [84].

- Reactive sputtering: this type of sputtering is based on chemical reactions between the sputtering gas and the target in the condensation phase at the surface of the substrate. The most sputter gas commonly used is either oxygen or nitrogen gas [85].

- Magnetron sputtering: includes not only the deployment of an electrical field, but also the use of a magnetic field for particle ejection from the target material and improves the rate of deposition. In this case, the operating pressure is lower than 4 Pa [83-85].

Among the main advantages of sputtering deposition is the production of relatively dense, continuous and smooth surface of thin films than chemical vapor deposition (CVD) as a result of rising surface mobility [82]. The stoichiometric amount is almost similar between the target and the sample surface during the deposition process. Sputtering allows a relatively fast deposition, good adhesion and the use of multiple targets per deposition in order to deposit complex material on the sample [82, 86].

Cho et al [87] deposited Zn(O,S) films at a constant amount of oxygen flux gas using reactive sputtering to analyze the effect of oxygen to sulfur composition ratio on the electronic properties. The deposition was realized by RF magnetron sputtering using ZnS as a target with a controlled mixed gas of 90% Ar/10% O_2 with a variation of the $O_2/(Ar+O_2)$ from 0 to 3.0% [87]. The pressure is set at 0.67 Pa with 166°C as a substrate temperature. The ratio S/(O+S) has changed from 1 to 0.16 with the increase of oxygen content in the mixed gas. Uniform and dense sputtered films were obtained for Zn(O,S) samples rich in oxygen content. All the Zn(O,S) films have exhibited a hexagonal wurtzite structure with a preferential orientation along the (112) plane and a thickness of 30 nm [87]. However, for Zn(O,S) with oxygen deficiency have been reported to have a $Zn(OH)_2$ secondary phase in the bottom region of the layer. It was recommended to use a plasma-induced phase distribution to increase the control of the composition profile anticipated [87].

Another case of RF sputtering deposition of Zn(O,S) thin film was reported by Grimm et al [88] using a mixed target of ZnS/ZnO as base material and argon as the sputtering gas. A commercial target was used with a S/(S+O) ratio of 0.4. The RF sputtering process was realized with 13.56 MHz frequency with a deposition rate of 50 nm/min and 3-9 x 10^{-6} bar as vacuum pressure. the RF sputtered Zn(O,S) samples deposited by Grimm et al [88] were compared with a previous study of Zn(O,S) films achieved by reactive sputtering in oxygen vacuum atmosphere [89]. The RF sputtered Zn(O,S) samples contained a low percentage of contamination by sulfate and hydroxide compounds unlike the reactive sputtered Zn(O,S) films. RF sputtered Zn(O,S) films were also found to be high in sulfur content with the increase of pressure inside the chamber. Additionally, the obtained Zn(O,S) films [88] from RF sputtering have demonstrated a uniform and compact layer with no additional secondary phase, improved crystallinity compared to reactive sputtered Zn(O,S) films and an efficiency of 14.5% for glass/Mo/Cu(In, Ga)(S, $Se)_2$ Zn(O,S)/ZnO:Al solar cell device structure [88].

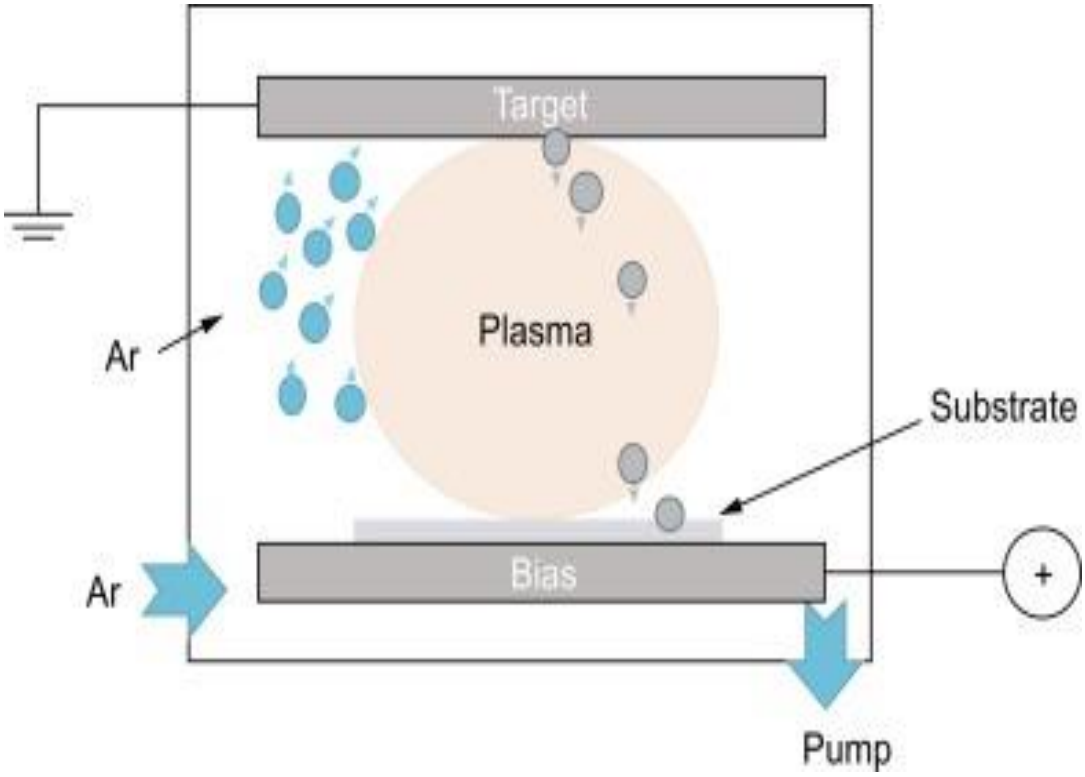

Figure 1.5: schematic illustration of sputtering deposition process [89].

In summary, the authors describe in their articles the sputtering process applied for the deposition of Zn(O,S) thin films. All the articles [85-90] mention the uniformity and high density of the Zn(O,S) layers with a high crystalline structure. The control

of temperature, pressure and S/(S+O) ratio values are also important to attain the desired results. However, it was stated that the reactive sputtered Zn(O,S) have exhibited contaminations, inhomogeneity of S/(O+S) ratio and oxygen deficiency can lead to non-uniform Zn(O,S) layer and can affect the electrical properties [88,90]. Other limitations are related to the cost and erosion of the target material, as well as flaking of the films under thermal stress containing undesirable particles which happen especially in DC and reactive sputtering [84, 91].

1.4.5 Pulsed laser deposition

Pulsed laser deposition (PLD) is one of the PVD methods that allow the stoichiometric transfer of the materials. PLD is used to deposit a number of non-sublimable materials (e.g. oxides, nitrides, carbides, etc.) [92, 93]. According to H. Fujioka [93], electromagnetic radiation from a highly intensive pulsed laser is used as an energy source, which is projected through an optical focus lens towards the surface a solid or liquid material which is called as "target" to evaporate this material in a vacuum chamber. The target material interacts with the laser beam and creates a plasma "plume" from the vaporized and ionized particles. The pressure inside the chamber is kept generally in the range of 10^{-11} to 10^{-6} Torr with the help of a vacuum pump [92, 93]. Also, PLD system (figure 1.6) allows introducing different types of gases inert or reactive (e.g. O_2, H_2, N_2 and Ar).

The plasma plume is composed of atoms, molecules, ions and electrons that are ejected from the target during evaporation. The extracted particles are deposited on the substrate surface as the result of condensation. The distribution of the elements extracted depends on the pressure applied inside the chamber and is close to the stoichiometry of the target material [94].

The quality of the deposited films depends upon the laser energy applied and the condensation rate of the particles on the substrate. When the rate of condensation is high enough, then there is a thermal equilibrium that is reached by the particles which will allow the nucleation and growth process on the surface. The layers growth is affected by several parameters that are important: laser parameters (wavelength,

pulse number, pulse energy, etc.), temperature and pressure, substrate surface morphology [93].

The usage of the PLD process has been mentioned in several reports, and several laser types have been used for thin film deposition. Such types of lasers can be classified into two categories: conventional and ultrafast PLD lasers [94]. The conventional PLD laser is usually based on UV excimer gas laser of nanosecond pulses duration with the average pulse energy in the range of 0.01-10 J/cm². So called XeCl, KrF, ArF, F_2 types of lasers can be applied with 308 nm, 248 nm, 193 nm, 157 nm wavelengths respectively [86,93]. On the other hand, the ultrafast excimer types lasers are such as CO_2 Nd:YAG laser (1064 nm wavelength) use a high electrical filed for the creation of the plasma plume discharge to increase the deposition rate to picoseconds or femtoseconds duration between each pulse. The average pulse energy employed is in the range of microjoules scale [92-95].

The most important advantages of this method are related to the following points:

- Relatively simple process and the operating parameters can be easily controlled inside the vacuum chamber [92].
- The rotation of the substrate while being heated make it possible to deposit uniform and compact layers [93-95]
- The PLD method makes it possible to control the stoichiometry of non-sublimable materials. After deposition, the thin film layer formed has a close stoichiometric amount to the target material [92].
- Possibility to increase the rate of deposition with higher pulse energy and frequency applied during the process [95].

- This method allows the deposition of various combinations of materials at once by using alloying/target mixture, in different kinds of atmosphere (inert or active) [94]. Therefore, the deposition of ternary, quaternary and other complex chemical compounds is possible.
- PLD deposition at lower temperatures prevents the deterioration of the thin film optoelectronic characteristic [92].

In contrast, the main limitations of PLD are:

- The method is relatively costly as the ultrashort pulsed laser types are not yet widely used by laboratories and industries [93].
- Formation of micro-sized droplets inside the deposited films may occur due to high intensity of the laser beam which results in an ejection of bigger particle sizes from the target material [95-98].
- The deposition is performed on a small substrate area as the impact spot of the pulsed laser beam is small [93, 96, 97].
- Incompatibility of certain material characteristics (such as reflectivity, absorption coefficient, etc.) with some types of lasers can occur [96].

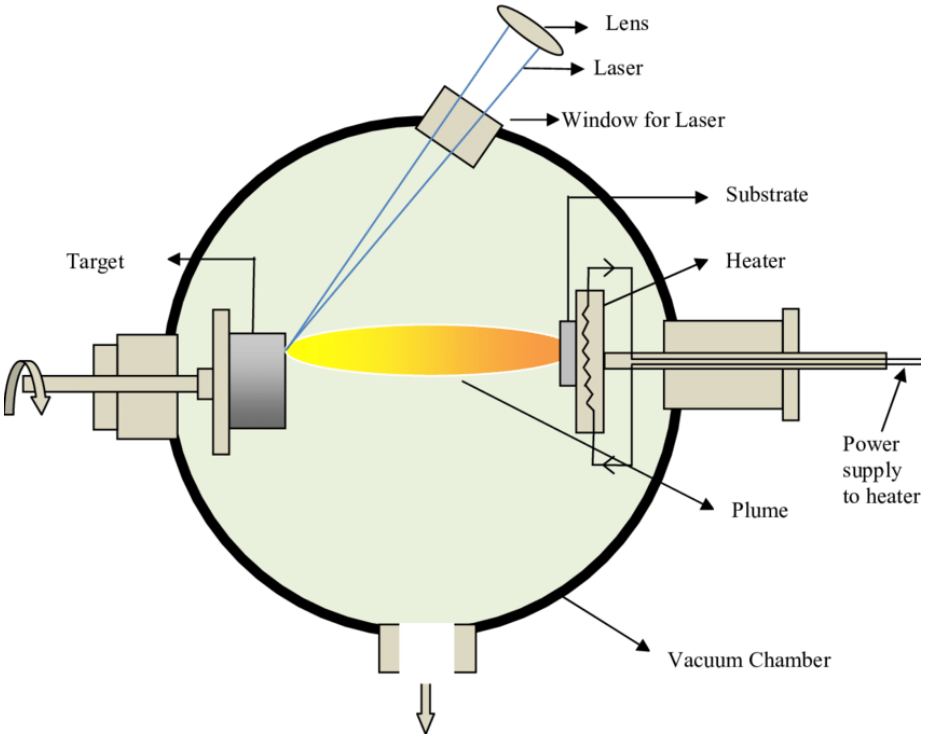

- Figure 1.6: schematic illustration of the pulsed laser deposition process [99].

Several studies have reported the influence of PLD parameters on the deposition of Zn(O,S) buffer layers. Deulkar et al [100] deposited Zn(O,S) layers by pulsed laser deposition method on a quartz substrate and investigated the optoelectronic characteristics of the films. The target used was the result of a sintered pellet by precipitation of zinc hydroxide and zinc sulfate solution. The target material was stated to be composed of partially oxidized ZnS cold-pressed at 2.6 x 10^6 Torr. the deposition was carried out in a vacuum chamber at different temperatures (in the range of 450 to 630°C) with a KrF excimer laser under the pressure of 2 x 10^{-7} Torr, 270 mJ as beam energy, 10 Hz as laser frequency and 30 min as deposition time. The structural analysis [100] shows that the deposited Zn(O,S) films by PLD have

been influenced mainly by the variation of temperature and stoichiometry of the plasma plume. The average grain size and roughness of the films were observed to be increasing with the rise of temperature from 450 to 630°C. Deulkar et al [100] confirmed the presence of sphalerite peaks for the Zn(O,S) samples shifting gradually by ~1° due to a decrease of the lattice parameter. As noted [100], this modification lattice spacing is caused by the substitution of sulfur by oxygen with the increase of deposition temperature. Lastly, the optical band gap was observed to be decreasing from 3.42 to 3.22 eV following the increase of oxygen content in the Zn(O,S) films.

Furthermore, PLD-grown Zn(O,S) buffer layers were prepared and characterized in a previous study achieved by our laboratory research group [101]. The PLD Zn(O,S) layers were produced using a 248nm KrF excimer laser beam focused on a rotating target surface of a commercial Zn(O,S) hot-pressed pellet. The deposition was carried out in high vacuum with a pressure of $3x10^{-6}$ Torr, 250 mJ beam energy, 7 Hz repetition rate [101]. The substrate temperature was varied from RT to 400℃. The cross-section analysis by SEM of the samples showed that all deposited Zn(O,S) layers have a thickness around ~650 nm, except for the sample deposited at 400°C which the thickness was found to be 580 nm. Moreover, morphological analysis [101] revealed that the obtained Zn(O,S) layers were found to be amorphous at room temperature and polycrystalline for temperatures above 100°C. The crystal structure of the Zn(O,S) films deposited at 200 to 400°C was identified as wurtzite Zn(O,S) phase oriented in the (002) plane. Whereas the film deposited at 100°C was found to have a mixture of ZnO-ZnS-Zn(O,S) phases. Through this study [101], it was shown that the deposition temperature of the films affects the elemental composition of the samples as well according to the EDX result. The increase of deposition temperature results in a decrease of sulfur content and increase of oxygen amount. The analysis of the films showed high optical transmittance and a band gap around 3.1 eV with no evident effect of deposition temperature [101]. However, for the temperatures higher than 300°C, a sharp increase in resistivity and the decrease of carrier mobility was observed. It was stated that this method can be optimal to produce TFSCs devices with Zn(O,S) as a buffer layer material[101].

In summary, the PLD method can affect the quality of Zn(O,S) film deposition upon the conditions used [92-101]. Several main advantages and drawbacks for the PLD

technique were mentioned by the authors [92-98]. In all reports[100-101], the deposition temperature is observed to affect mainly the composition, crystal structure and electric properties of the Zn(O,S) films.

1.4.6 Other deposition methods

In recent studies, other deposition methods [102-104] were employed to form the Zn(O,S) films in the laboratory scale in order to study their properties and performance with TFSCs device. Cheng et al [102] deposited Zn(O,S) layers using an electrodeposition method to investigate the effect of tartaric acid on the film's optoelectronic characteristics. A potentiostatic electrodepositing technique was applied with a chemical solution precursor including zinc sulfate, sodium thiosulfate and different concentration of tartaric acid as complexing agent [102]. The Zn(O,S) layers were formed on FTO substrates at a voltage of 1.1 V on working electrode (vs. Ag/AgCl reference electrode). Uniform and dense Zn(O,S) films were formed with a thickness of ~200 nm and roughness of <20 nm for all deposited layers. Fast nucleation and high crystal structure quality was obtained with the increase of tartaric acid concentration [102]. The optical transmittance was shown to be decreasing following the lower concentration of tartaric acid. Optical band gaps of the Zn(O,S) films were estimated to be between 3.3 and 3.5 eV [102]. Cheng et al [102] conclude that the use of tartaric acid in the Zn(O,S) film electrodeposition contributes to reduce the cathodic polarization, oxidation and increase the quality and the controllability of films.

Zhang et al [103] deposited Zn(O,S) buffer layers using ozone assisted photochemical deposition (PCD) method and studied their properties. The solution used for the deposition contained zinc sulfate, sodium sulfite and sulfuric acid as precursors. The deposition was carried out at 60°C by immersing Mo substrates on the solution before being irradiated with a UV lamp. The ozone flow rate was varied to study the influence on the Zn(O,S) films. According to the authors [103], the morphological analysis reveals no presence of large-sized particles and good surface coverage with a thickness of 40 nm for all obtained films. The Zn(O,S) films also exhibit an average optical transmittance of 80% in the range of 350-800 nm

wavelength. It was found that the optical band gap of the Zn(O,S) films have decreased from 3.7 to 3.4 eV with an increase of ozone flow rate. Zhang et al [103] observed that the application of these films exhibited a conversion efficiency of 3.0% with V_{oc}= 0.516 V, J_{sc}=16.8 mA/cm², FF=34.46% in a CZTS solar cell structure.

In a study done by Merike Kriisa et al [104] (TalTech), an investigation was performed on the optoelectronic properties of deposited Zn(O,S) by aerosol assisted chemical vapor deposition (AACVD). The deposition of Zn(O,S) layers was carried at 225°C during 20-30 min using nebulized zinc(II)acetylacetonate solution by an ultrasonic atomizer. Nitrogen as carrier gas (between 5 and 7 L/min flow rate) and H_2S as reactant gas (flow rate between 0 and 20 mL/min) through the aerosol stream [104]. XRD analysis performed shows that the samples have a polycrystalline structure close to hexagonal ZnS and ZnO. It was observed that the increase of H_2S gas flow rate above 2 mL/min leads to an inhomogeneous Zn(O,S) morphological structure [104]. Therefore, the optimal gas flow rate values for uniform and homogeneous Zn(O,S) layers were determined to be 2 mL/min of H_2S and 5 L/min of N_2. The average optical transmittance was around 70% with a band gap of 3.6 eV [3]. Efficiency values were between 10.9 to 15.4% with a CIGSSe solar cell device, which indicates a slight improvement compared with reference CdS buffer layer solar cell performance.

In conclusion, the reports [102-104] show that it is possible to deposit the Zn(O,S) thin films using other techniques of deposition such as electrodeposition and aerosol assisted chemical vapor deposition. The optoelectronic characteristics described in these papers [102-104] are close to the Zn(O,S) thin film properties obtained by the deposition methods described before [56-101]. However, the film thickness has also an effect on the Zn(O,S) films properties, which will be discussed in part 1.5.

1.5 Thickness effect of Zn(O,S) thin films

Similarly, in addition to the temperature and the composition ratio effect on Zn(O,S) buffer films properties described before in part 1.2, the thickness also influences the

optoelectronic properties of Cd-free buffer layers as reported [105-109]. Hong et al showed [105] the effect of Cd-free film thickness on the structural and optical characteristics. The film thickness obtained was in the range of 24 to 50 nm. It was demonstrated that the increase of film thickness has no effect on the crystal structure. The band gap has been reduced from 3.24 to 3.12 eV with the increase thickness from 24 to 50 nm. The optical transmittance for all obtained samples was above 80% in the visible range of spectrum with a shift towards longer wavelengths following the increase of film thickness [105].

Furthermore, there have been some reports about the thickness effect of the Zn(O,S) buffer layers on the optoelectronic properties and the performance of some complete TFSCs devices:

Sun et al [106] investigated the thickness effect of the Zn(O,S) deposited layers by CBD on the optoelectronic properties. The deposition was performed in a chemical bath solution containing zinc acetate, thiourea and deionized water. The deposition temperature was about 85°C with different immersion time (from 12 to 25 min) to achieve a variation of film thickness from 20 nm to 50 nm. SEM analysis of the deposited Zn(O,S) films shows formation of a dense and uniform surface. The UV-Vis analysis shows the optical band gap decrease from 3.75 to 3.4 eV with the increase of the film thickness from 20 to 50 nm respectively. The authors [106] explain the thickness effect as related to S/(S+O) ratio according to Bär et al interpretation [107]. An increase in the film thickness results in an increase of incorporation of oxygen in the Zn(O,S) structure. Therefore, it was observed that the S/(S+O) ratios decreased with the increase of the thickness which resulted in reducing the optical bandgap values (shift of absorption edge to longer wavelengths). It was also reported by Sun et al [106] that the thinner CBD Zn(O,S) layer (20 nm) contains lower defects density compared with 50 nm thick Zn(O,S) layer. As a result, the recombination rate of the CIS solar cell device increased with an increase in the thickness of the Zn(O, S) film.

In a recent study, Choi et al [50] used the ALD method to prepare Zn(O,S) films with different thicknesses. The ALD Zn(O,S) films were deposited at 120°C using nitrogen as a purging gas and a different number of cycles to achieve desired thicknesses and composition. The S/(S+O) ratios of the Zn(O,S) layers were found to be between 0.10 and 0.25 and the film thicknesses between30 and 140 nm, respectively. Also, The band gap decreased from 3.2 to 2.9 eV following the increase

of Zn(O,S) film thickness. Choi et al [50] observed that the optimal rate of deposition is 29 nm/cycle for a uniform and high-density Zn(O,S) layers. Additionally, it was noticed that the increase of Zn(O,S) film thickness from 30 to 140 nm lead to a decrease of Jsc and FF values in complete CIGSSe solar cell device.

Shi et al [108] deposited Zn(O,S) films using the sputtering method and tried to investigate the thickness dependence on the properties of the layer structure. They also tried to find the optimum value of film thickness based on the results obtained for the performance of the CIGS solar cell device. The Zn(O,S) layers were formed by radio frequency (RF) sputtering using 100 W power with a background pressure of 0.8 Pa and 150°C temperature. The Zn(O,S) film thickness was varied from 20 to 240 nm and SLG/Mo/Cu(In,Ga)Se_2/Zn(O,S)/Al–ZnO /Ni-Al was used as TFSC device to study the performance of the samples with the thickness variation from 20 to 100 nm. The results showed that all Zn(O,S) films have an oxygen to sulfur ratio of 0.58, which indicates that the composition was not affected by the increase of film thickness. The morphology of Zn(O,S) films shows dense and uniform surface structures in which the roughness increases with the increase of film thickness [109]. However, there was confirmation of the presence of defects within the samples obtained. It was concluded that the decrease of film thickness for the sputtered Zn(O,S) films results in an increase of defect density. The authors [108] demonstrated that these defects can lead to carrier trapping inside the Zn(O,S) layer with the increase of film thickness, which affects on the electrical properties. Additionally, the increase of defect density resulted in poor CIGS solar cell device performance and an increase of interface recombination rate. Finally, the CIGS solar cell device attained an efficiency of 12.5 % with a thickness of 50 nm thick Zn(O,S) film according to Shihan et al report [108].

Another study certified by the national renewable energy laboratory (NREL) was for Zn(O,S) buffer layers deposited by CBD method with a variation in film thickness and temperature performed by Ramanathan et al [109]. Deposited Zn(O,S) films were achieved by an aqueous chemical bath that contains a solution of zinc sulfate with thiourea and ammonium hydroxide at different deposition time and temperatures (65-95°C) for each layer. The obtained CBD Zn(O,S) films have a thickness that varies from 20 to 30 nm[109]. The increase of thickness resulted in a decrease of the fill factor (From 76 to 71%) and efficiency (16.5 to 15.1%) with a CIGS solar cell device [109].

1.6 Summary of literature Overview

According to the literature review, the choice of the buffer layer material affects seriously on the performance of the solar cell device. Although the manufacturing of TFSCs with CdS buffer layers has been so far widely used, there were some concerns for the parasitic-absorbing properties and the impact on the environment of the CdS films [30-33]. The authors have demonstrated that Zn(O,S) as relatively new Cd-free buffer layer has promising optoelectronic characteristics to replace the CdS buffers in complete SC structures. Examples of promising Zn(O,S) properties are a wider band gap, low toxicity and earth abundance. It was confirmed that an efficiency of 21% could be attained for CIGS solar cell with Zn(O,S) buffer layer [35]. In the last decades, the Zn(O,S) thin films have been deposited using several techniques such as chemical bath deposition, spray pyrolysis, atomic layer deposition, sputtering and pulsed laser deposition [56-104]. Each deposition method is employed with different conditions that can influence positively on the quality of Zn(O,S) film such as a good surface coverage, conservation of stoichiometry, improvement of electrical properties and solar cell performance, etc. In contrast, inhomogeneous structure, non-uniformity, risk of contamination of the layers are among the examples of drawbacks that could occur. Moreover, some other new deposition methods of Zn(O,S) layers preparation have been reported by several groups [102-104]. For most of the authors mentioned in the literature review, they obtained Zn(O,S) layers with n-type of conductivity, bandgap value in the range of 2.6-3.75 eV and PCE in the range from 8 to 21% with different solar cell devices with Zn(O,S) buffer layers.

Additionally, there have been several reports that describe the variation effect of sulfur to oxygen ratio, annealing atmosphere, deposition temperature among other effects on the properties of Zn(O,S) layers reported in the literature [43-55]. However, the thickness effect on the optoelectronic characteristics Zn(O,S) film has not been completely explored, as no previous research group has reported the thickness effect for the properties of PLD Zn(O,S) layers. Hence, based on the

previous paper published by our group [101], the present study is focused to examine the change of the composition, crystal structure, morphology, optical and electrical properties of Zn(O,S) thin films prepared by PLD with the change of film thickness.

1.7 Aim of study

The purpose of this study is to achieve the following aims that include:

- To deposit Zn(O,S) thin films at 300 °C in high vacuum with different thickness (130, 210, 280 and 330 nm) by pulsed laser deposition (PLD) method.

- To investigates the thickness effect on structural, morphological, optical and electrical properties of obtained Zn(O,S) layers.

2. EXPERIMENT PROCEDURE AND ANALYSIS

2.1 Technical parameters of pulsed laser deposition system

All depositions were performed by using the Nocera Pioneer 120 PLD system equipped with KrF excimer laser Coherent Compex 102 F (248 nm wavelength) as shown in figure 2.1. The system gives possibilities to deposit high quality layers of sublimable and non-sublimable materials (ceramics etc.) onto rotated and heated substrates in high vacuum and in controllable process gas atmosphere (N_2 or O_2). The technical parameters of the Nocera Pioneer 120 PLD system are mentioned in the following points:

- Substrate temperature can vary from RT to 900°C.
- Operating pressure range: from $5 \cdot 10^{-7}$ Torr to 500 mTorr.
- Laser specifications: 248 nm UV excimer laser, maximum pulse energy till 400 mJ. 20 Hz maximum repetition rate, 6 W maximum average power, 20ns pulse duration.

Figure 2.1: photograph image of Neocera Pioneer-120 PLD system.

- The target material can be prepared as a hot-pressed pellet or as a sintered pellet with a minimal diameter around 12 mm and with the thickness in the range 1-30 mm.
- Substrate cleaning is necessary before deposition in order to avoid impurities
- Maximal square substrate size can be 36.5 mm for one substrate or 9.5 mm for five substrates. Another alternative variant is one round substrate with a diameter of 50.8 mm with semiconductor flat.
- Optimal substrate thickness is around 1 mm.

2.2 Glass substrates and Zn(O,S) target preparation

The quality of the deposition depends greatly on the cleanliness of the substrate. Cleaning is necessary to remove all traces of grease and dust. It's important to make sure that the surface of the substrate does not have any scratches or defects. These conditions are essential for the good adhesion and thickness uniformity of the deposited films on the surface of substrate [110]. For this study, soda-lime glass substrates (SLG), 2 x 2 cm in size, were prepared and a multi-step cleaning process was employed. First, the substrates were ultrasonically cleaned for 15 min in 20% solution of Decon 90 and in deionized water at 50℃ respectively. This stage is important for extracting traces of grease and impurities from the glass surface [110].

Filtered air flow was used to dry the SLG substrates with following exposition for 15 min in the Nova Scan Optical UV-Ozone cleaning system. This process eliminates traces of organic contaminations from the substrate surface by photo-sensitized oxidation. Organic molecules are excited and dissociated by the absorption of short wavelength UV following an oxidation by photo-induced ozone [111].

In this research, the Testbourne Ltd. hot-pressed target of 25.4 mm diameter × 6 mm thickness was used for the deposition of Zn(O,S) layers by PLD. The Zn(O,S)

pellet was prepared by mechanical mixture of 75 at.% ZnO and 25 at.% ZnS fine powders with following hot-pressing.

2.3 Pulsed laser deposition of Zn(O,S) thin films

The deposition of Zn(O,S) thin films with different thicknesses was performed using the Neocera Pioneer 120 PLD system in high vacuum according to technology reported in the previous study of our lab [101]. The pressure in the vacuum chamber during the deposition was around 3×10^{-6} Torr. A distance of 9 cm was applied between the target and the glass substrates. For all layers, the deposition conditions were practically identical (substrate temperature was 300℃, the laser pulse energy was 250 mJ, the repetition rate was 7 Hz and the laser beam was focused on the target with a spot size of ~5 mm^2) to prepare adhesive, dense and uniform Zn(O,S) layers. To achieve uniformity of the film thickness rotating of the substrate has been applied. Table 2.1 shows the deposition time vs. film thickness for obtained Zn(O,S) films.

Table 2.1: deposition time and pulse numbers based on the Zn(O,S) layers thickness.

Deposition time (min)	Laser pulses number	Film thickness (nm)
25	11692	130
35	17538	210
48	23385	280
58	29231	330

2.4 Characterization of Zn(O,S) films

Deposited Zn(O,S) layers have been characterized by instrumental techniques to study the morphology (HR-SEM), crystal structure (XRD), chemical composition (EDX), optical and electrical properties (UV-Vis spectroscopy and Hall effect measurements) of the films. In this section, the descriptions of each characterization technique are introduced briefly.

2.4.1 XRD analysis

The structural composition of Zn(O,S) thin films was investigated using X-ray diffraction (XRD) method. XRD analysis was performed by Rigaku Ultima IV diffractometer equipped with CuKα radiation source using the Bragg - Brentano (θ-2θ) geometry. Crystallites size was evaluated using Sherrer equation (1) [112]:

$$D = \frac{0.94\lambda}{\beta cos\theta} \qquad (1)$$

Where D is the average size of the crystallite in nanometres (nm), λ is the wavelength of X-ray radiation (1.5406 Å), θ is the Bragg angle in degrees (deg), and β is the full width at the half maximum (FWHM) of the peak positioned at the 2θ in the radians (rad).

The equation of Bragg's law (2) allows the calculation of interplanar spacing with an order of diffraction n=1 [112]:

$$d = \frac{\lambda}{\beta cos\theta} \qquad (2)$$

Where d is the interplanar spacing in nanometres (nm).

2.4.2 HR-SEM

ZEISS FE-SEM Ultra 55 high resolution scanning electron microscope (HR-SEM) was used for examination of the surface morphology, cross-section view and elemental composition of the obtained layers. SEM creates images of the sample surface that

are produced by using an intensive scanning electron beam. The electron beam is generated by acceleration and focusing of electrons which interact with the sample and the kinetic energy carried is dissipated. The analysis is accomplished through scanning the backscattered electrons (BE) (contains data about the composition) and secondary electrons (SE) (gives information about the morphology i.e. micrograph). It's a relatively low-destructive technique that allows for the material to be analyzed several times [113].

For our HR-SEM studies, the acceleration voltage was set about 4.0 kV (In-lens SE detection). The Bruker ESPRIT system 1.82 was applied for the purpose of determination of the elemental composition of the Zn(O,S) films using energy-dispersive X-ray spectroscopy (EDX). In this case, the accelerating voltage of Bruker ESPRIT system was calibrated at 7 kV [114].

2.4.3 UV-VIS spectroscopy

Optical properties (transmittance spectra) of Zn(O,S) thin films were measured in the wavelength range of 300 – 1000 nm by using Shimadzu 1800 UV-Vis spectrophotometer. The working principle of ultraviolet-visible spectrophotometry (UV-Vis) is based on the energy absorption in material from a light source which leads to an excitation of electrons and a transition from the ground state (low energy level) to higher energy state [115]. The contemporary double-beam UV-Vis instrumentation includes UV-visible light source, detector measuring the optical transmittance and two cells for the purpose of allowing the light to pass through. The promotion of electronic transition requires the interaction of short wavelength with high energy radiations available in the UV light (200-400nm;3.099-6.166 eV) with the visible range of the electromagnetic spectrum (400-800nm;3.099-1.544 eV) [115]. The detector also programmed to use a function of wavelength to allow the calculation of the absorption coefficient by the means of the following equation (3) [101,116]:

$$\alpha = 2.303 \times \log(\frac{T}{d}) \qquad (3)$$

Where α being the absorption coefficient, T is the optical transmittance in %, d is the layer's thickness in nm.

The optical band gap result of the samples were measured using Tauc equation (4) by plotting $h\nu$ versus $(\alpha h\nu)^2$. and extrapolating the linear part of the plot and taking the intercept with $h\nu$ axis (x axis) [116] represented in figure 3.5.

$$\alpha h\nu = A(h\nu - E_g)^n \quad (4)$$

Eg is the band gap value in eV, $h\nu$ is the energy of incident photons and n is an exponent that varies depending on type of transitions (e.g. n=0.5 for allowed direct electronic transitions).

2.4.4 Hall effect measurement

The electrical properties of the deposited Zn(O,S) films were investigated at room temperature (RT) using the variable temperature of MMR's Hall System and a Hall van der Pauw controller H-50. The four-probe contact system of van der Pauw geometry was applied using indium as a low resistive ohmic dot contact material on the surface of Zn(O, S) films. Four contacts (indium electrodes) were positioned on the sample and the Hall measurement was done by maintaining the current value constant through the electrode and a magnetic field is applied with magnetic induction in order to obtain the Hall effect [117]. Consequently, the obtained results show the data about electrical resistivity, mobility and carrier concentration within thin films.

3. RESULTS AND DISCUSSION

3.1 XRD analysis

Figure 3.1 represents XRD diffractogram of Zn(O,S) films deposited at 300°C with different film thicknesses of 130, 210, 280 and 330 nm. The XRD pattern showed a single peak around ~33.12° for all deposited films. As confirmed previously [101] by comparing the XRD peak of pure cubic (111) ZnO phase (PDF No: 01-075-1534) appeared at 33.50° and XRD peak of pure hexagonal (200) ZnS phase (PDF No: 01-079-0208) appeared at 33.05° the singular sharp peak at 33.12° is identified as the (002) diffraction peak of wurtzite Zn(O,S) phase [101]. In addition, the XRD profile indicates that deposited Zn(O,S) films exhibit a polycrystalline structure. Also, there is no presence of impurities or secondary phases within the films in frames of accuracy of the XRD technique.

3.2 Surface morphology and compositions

Figures 3.2 and 3.3 shows HR-SEM micrographs of the surface and cross-section views of the Zn(O,S) films deposited on a glass substrate at 300°C. The films are uniform, compact and well adherent to the substrate surface. The layers demonstrate a grainy structure in good agreement with the XRD results. Moreover, there is no visible cracks or pin-holes observed in the surface of all Zn(O,S) films formed. The SEM cross-sectional micrographs show the following thickness values for deposited layers: 130 nm, 210 nm, 280 nm, 330 nm (table 3.1).

Additionally, the grain size values were determined using the scale bar, taking into account the HR-SEM micrograph magnification shown in Figure 3.2. the average grain size of the films increased from 25 nm to 62 nm with the increase in film thickness (see table 3.1).

The EDX analysis reveals that there is a negligible fluctuation in the elemental composition with the increase of film thickness. The Zn(O,S) films have an average

atomic ratio of 46 at% zinc, 45 at% oxygen and 9 at% of sulfur content (with taking into account accuracy of EDX around +/- 0.5 at% in average).

The increase in film thickness is related to the increase in deposition time i.e. laser pulses number. Moreover, the interpretation of grain size growth is related to the interaction of vaporized atoms with the substrate as described in [118-123]. These interactions improve the recrystallization as a result of grain coalescence and surface diffusion with the increases of film thickness [118]. Furthermore, grain size growth is connected to longer heat exposure correspond to longer deposition time. This comes in agreement with what described in the previous study [101].

Table 3.1: The grain size and band gap values for deposited Zn(O,S) layers.

Film thickness (nm)	Average grain size (nm)	Band gap eV
130	25	3.00
210	31	2.98
280	48	2.97
330	62	2.96

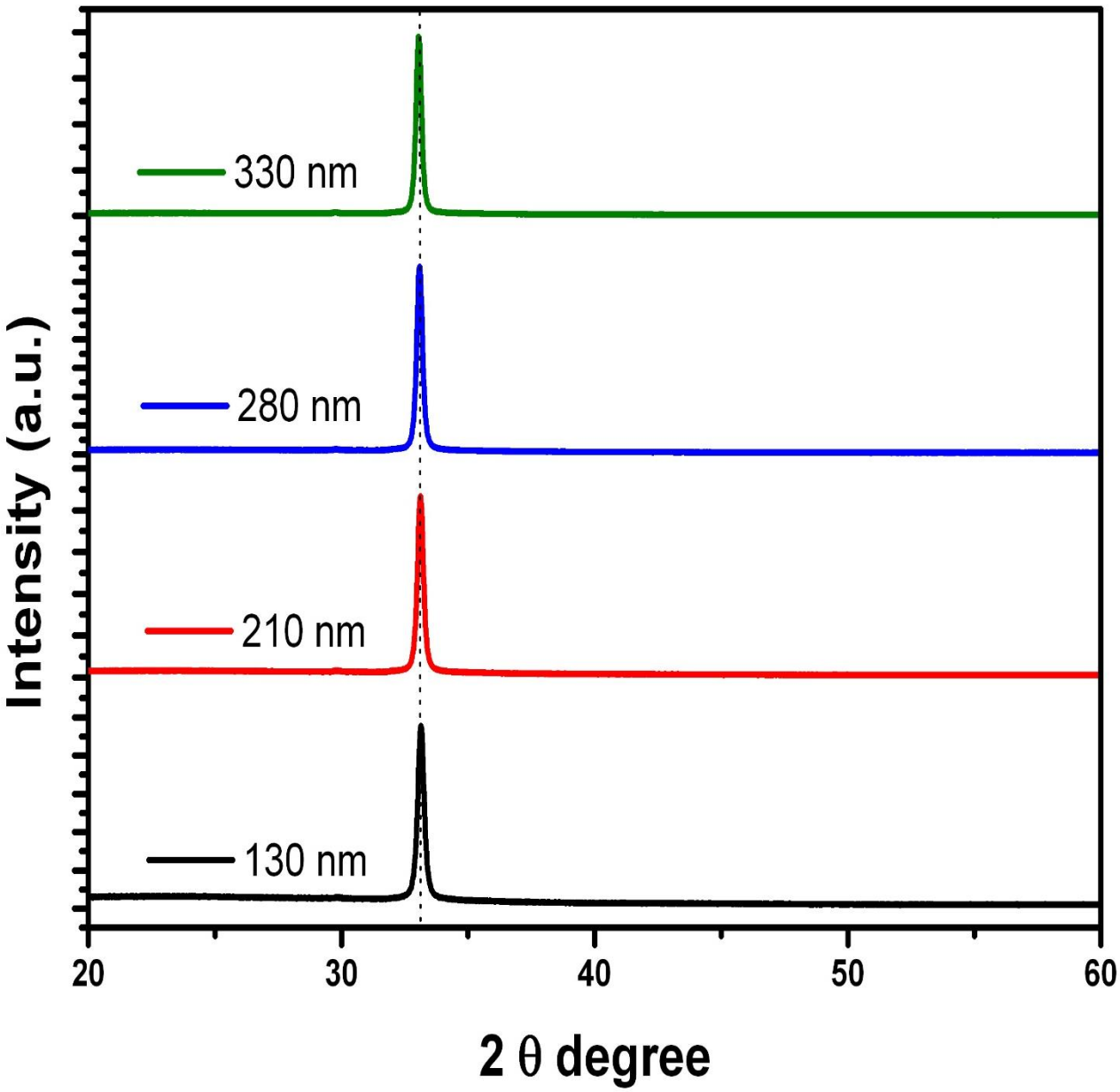

Figure 3.1: XRD patterns of Zn(O,S) films deposited at 300°C with different thickness of 130-330 nm.

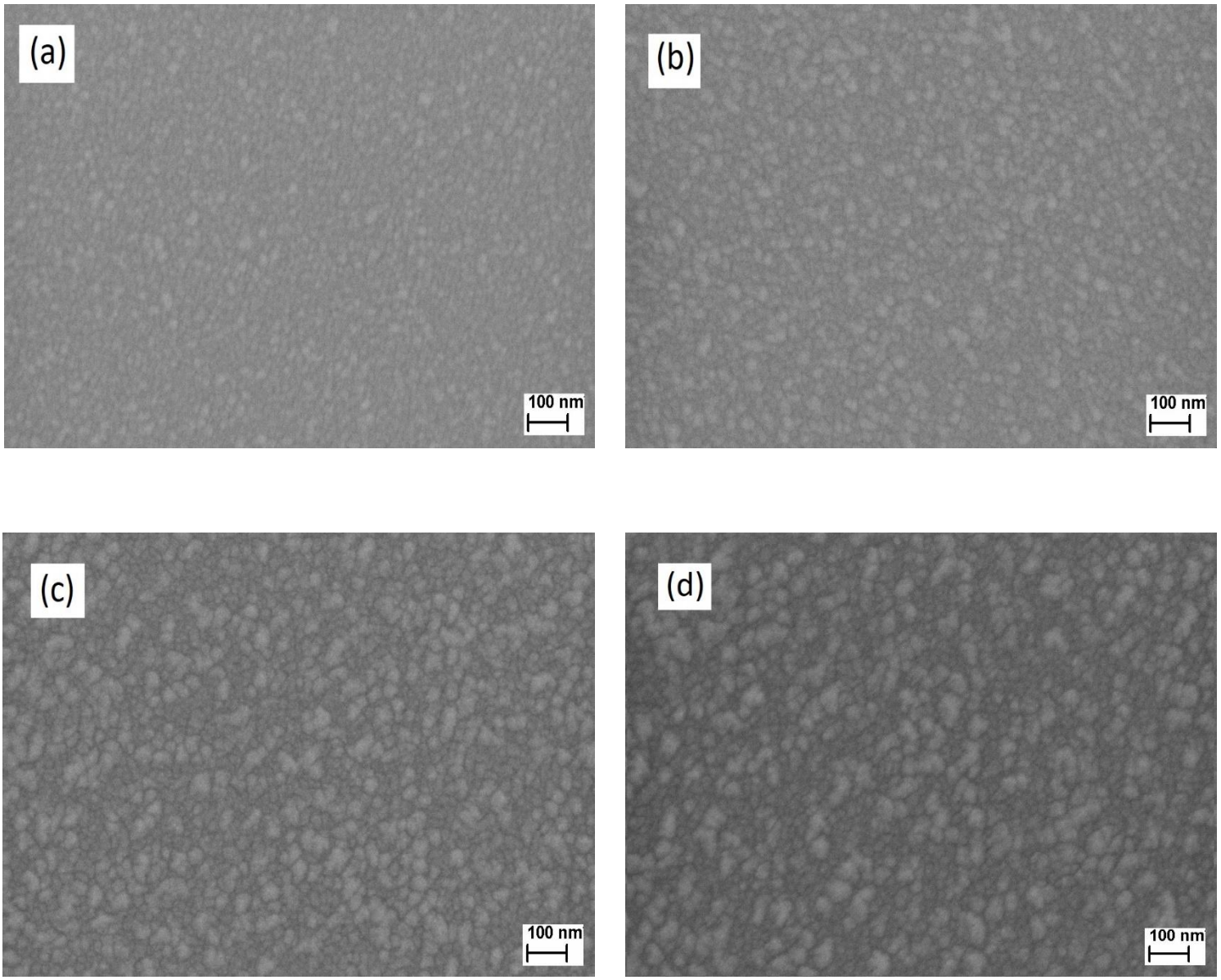

Figure 3.2: HR-SEM surface images of Zn(O,S) films deposited at 300°C with different thickness (a) 130 nm, (b) 210 nm, (c) 280 nm, (d) 330 nm.

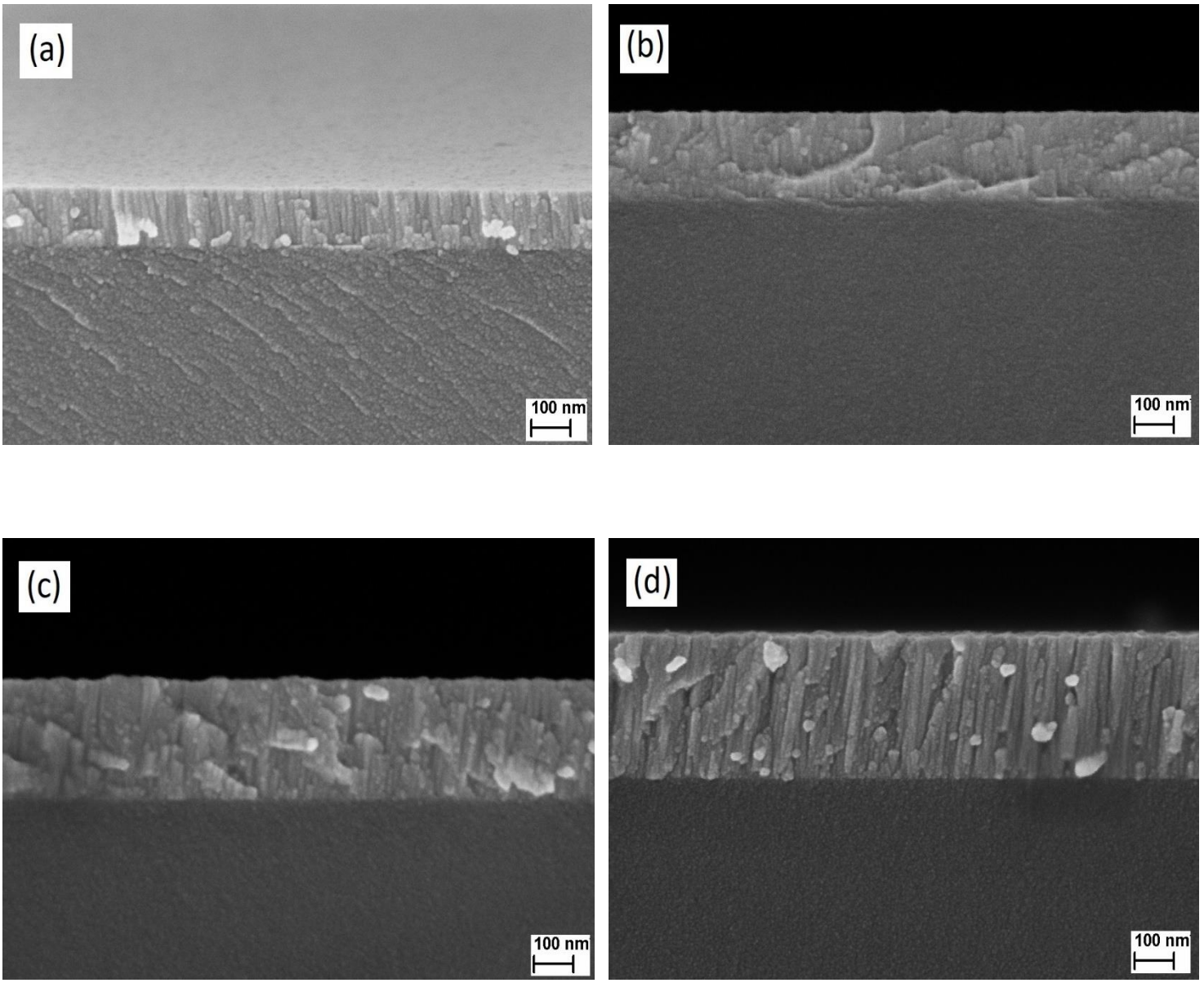

Figure 3.3 : HR-SEM cross-sectional images of Zn(O,S) films deposited at 300°C with different thickness (a) 130 nm, (b) 210 nm, (c) 280 nm, (d) 330 nm.

3.3 Optical analysis

Figure 3.4 shows the optical transmittance spectra of the Zn(O,S) films with different thicknesses. All Zn(O,S) films are relatively transparent in the visible range, with average transparency around ca. 85%. With the increase in film thickness, the absorption edges shifted to longer wavelengths from 400 to 450 nm. The gradual shift of the optical transmittance in figure 3.4 could be attributed to optical scattering due to the presence of possible defects (e.g. voids, oxygen or sulfur vacancies, planar defects, etc.) and change of grain boundary area throughout the formation of the obtained layers [120]. This supports the results of optical transmittance obtained from figure 3.4.

Tauc equation (4) was used to calculate the values of the band gaps shown in figure 3.5 for all the thicknesses. According to the figure 3.5, there is a slight decrease in optical band gap values from 3.0 eV to 2.96 eV with the increase in thickness from 130 to 330 nm as shown in table 3.1. In addition, according to the previous research by our group, the UV-vis analysis of the deposited Zn(O,S) films[101] reveals that the temperature variation from 200 - 400°C resulted in a band gap value of about 3.1 eV, which is close to the present study. The increase in film thickness resulted in nearly identical optical band gap values around 2.9 eV.

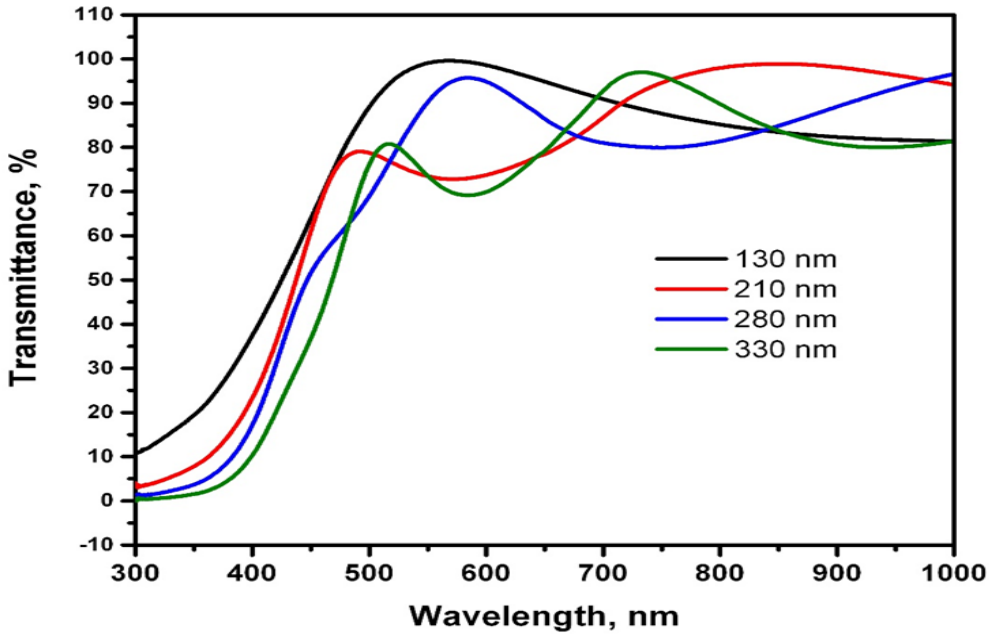

Figure 3.4: Transmittance spectra of Zn(O,S) films deposited at 300℃ with different film thickness of 130-330 nm.

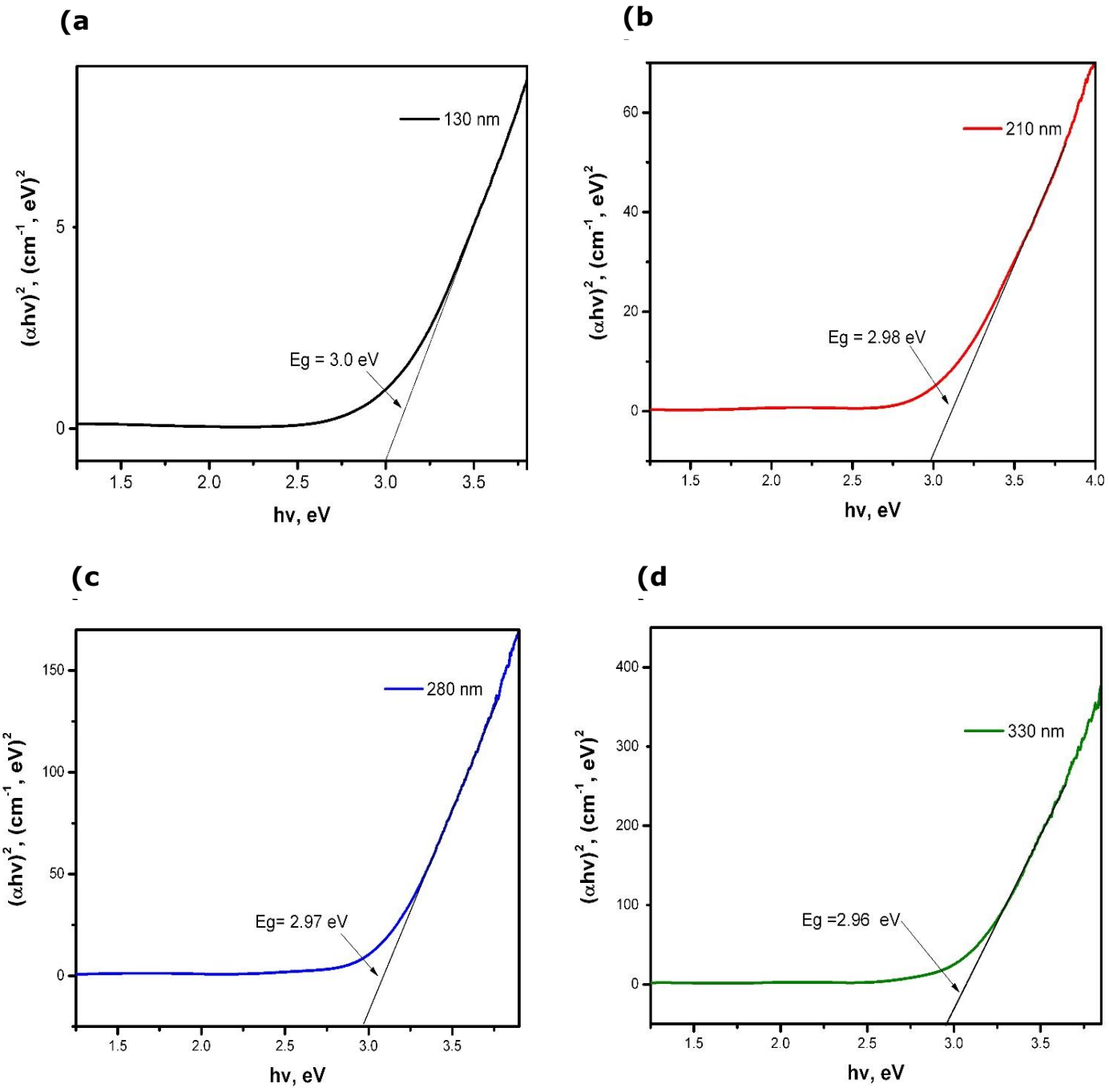

Figure 3.5: Optical band gaps of Zn(O,S) films deposited at 300°C with different thickness (a) 130 nm, (b) 210 nm, (c) 280 nm, (d) 330nm.

3.4 Electrical properties

Table 3.2 shows the Hall effect measurements of Zn(O,S) films deposited at 300°C with different film thicknesses of 130 - 330 nm. The sign of the Hall coefficient has revealed that electrons are the majority carriers, which correspond to an n-type conductivity of the films.

According to the results represented in table 3.2, it can be seen that all measured electrical parameters are very similar for prepared Zn(O,S) layers with different thickness. Therefore, it is not "bottle neck" for practical application of PLD Zn(O,S) for the structures with different thickness of buffer layer. All layers demonstrate relatively high values of electrical conductivity and charge carriers mobility with concentration of charge carriers of order 10^{19} cm^{-3}.

Table 3.2 : Electrical properties of the Zn(O,S) films deposited at 300°C with different films thicknesses of 130 –330 nm.

Film thickness (nm)	Resistivity (Ω·cm)	Carrier concentration (cm^{-3})	Carrier mobility ($cm^2/V{\cdot}s$)
130	0.38	2.11×10^{19}	0.78
210	0.39	1.96×10^{19}	0.82
280	0.40	2.62×10^{19}	0.60
330	0.51	1.9×10^{19}	0.60

Hall effect measurements error is ± 1%.

4. CONCLUSIONS

Polycrystalline conductive and optically transparent Zn(O,S) thin films with different thickness from 130 nm to 330 nm were deposited by PLD onto SLG substrates at 300°C. The study of morphology, phase and elemental composition, optical and electrical properties of obtained layers was performed with special account to film thickness effect. The obtained results of the films thickness variations effect on the Zn(O,S) films properties indicate the following:

- The XRD profile shows a singular diffraction peak around 33.12° for all Zn(O,S) films. The structural analysis revealed that there is a formation of polycrystalline ternary compound within the wurtzite crystal structure.
- HR-SEM micrographs show that all Zn(O,S) films exhibit a uniform and compact morphology with no visible crack or pinhole observed. The morphology analysis indicates that there is a growth of average grain size from 25 to 62 nm with the increase of film thickness from 130 to 330 nm. This increase both in thickness and grain size was attributed mainly to longer deposition time, surface diffusion and coalescence of the grains.
- According to EDX analysis, a negligible fluctuation of elemental composition in obtained layers was observed.
- It was found, that the optical band gap is decreasing slightly from 3.0 to 2.96 eV with the increase of film thickness.
- The Hall effect data confirm that all Zn(O,S) layers exhibit n-type of conductivity and all measured electrical parameters are very similar for prepared Zn(O,S) layers with different thickness. All layers demonstrate relatively high values of electrical conductivity and charge carriers mobility with concentration of charge carriers of order 10^{19} cm^{-3}.

It should be noted, that thickness effect is not significant from the point of view of electrical and optical properties of Zn(O,S) layers prepared by PLD in the thickness range from 130 to 330 nm. Based on the results found in this study along with already available in the literature, it can be concluded, that the Zn(O,S) thin film is a prospective candidate to replace the toxic CdS buffers in complete solar cell structures with different configuration and thickness.

SUMMARY

In the last decade, a lot of attention has been devoted to enhancing the PCE of thin film solar cells. The performance of these solar cell devices is based on the choice of the functional layer materials and microstructures. The choice of the optimal buffer layer is one of the key factors influencing the solar cell PCE. Moreover, development of low toxic Cd-free buffer layers is very actual task for thin film solar cells technology. According to the literature data, the Zn(O,S) is a low toxic n-type semiconductor with a band gap in the range of 2.6-3.7 eV and with achieved PCE of complete solar cell structures in the range from 8 to 21% i.e. Zn(O,S) films is a promising candidate to replace CdS buffer layers in complete solar cell structures.

The present thesis is focused on comparative study of the Zn(O,S) thin films deposited by PLD with different film thickness. The main purpose was to investigate the thickness effect on structural, morphological, optical and electrical properties of deposited layers.

All films were deposited onto the SLG substrates at the temperature of 300°C in high vacuum using a hot-pressed target containing a mixture of 75 at% of ZnO and 25 at% of ZnS fine powders with variation of deposition time from 25 to 58 min to obtain film thickness from 130 to 330 nm. The characterization results show that the variation of film thickness has minor effect on the morphology and crystal structure of the grown films. The XRD patterns confirm the presence of a ternary Zn(O,S) compound phase with hexagonal wurtzite structure. The HR-SEM micrographs show that the all prepared films are uniform with dense structure and demonstrate adhesive coherence to glass interface with absence of visible cracks or pinholes. It was found that the grain size increased with increase of film thickness. The optical bandgap values were calculated on the basis of electron spectra with average value close to 3 eV for all deposited layers without significant deviations. The Hall effect measurements show relatively low resistivity of prepared Zn(O,S) layers in the range from 0.38 to 0.51 Ω·cm with an increase of film thickness and a carrier concentration of order 10^{19} cm^{-3}, carriers mobility around 0.7 $cm^2/V{\cdot}s$ and n-type of conductivity. Findings show, that all obtained layers demonstrate uniform adhesive polycrystalline structure with quite similar optical and electrical parameters and can be potentially applied as buffer layers in complete Cd-free solar cell structures.

LIST OF REFERENCES

[1] Zhu, K., & Jiang, X. Slowing down of globalization and global CO2 emissions. Energy Economics, 84 (2019) 104483. DOI : 10.1016/j.eneco.2019.104483

[2] Mahjabeen, Shah, S. Z. A., Chughtai, S., & Simonetti, B. Renewable energy, institutional stability, environment and economic growth nexus of D-8 countries. Energy Strategy Reviews, 29 (2020) 100484. DOI:10.1016/j.esr.2020.100484 .

[3] Sørensen, B. (Energy system planning. Renewable Energy. (2017) pp. 649–850. DOI:10.1016/b978-0-12-804567-1.00006-2r.

[4] Martinez-Gracia, A. Solar energy availability. Solar Hydrogen Production. (2019)113–149. DOI:10.1016/b978-0-12-814853-2.00005-9.

[5] Breeze, P. Solar Photovoltaic Technologies. Solar Power Generation. (2016) pp. 51–55. DOI:10.1016/b978-0-12-804004-1.00008-7.

[6] Green, M. A., Dunlop, E. D., Levi, D. H., Hohl-Ebinger, J., Yoshita, M., & Ho-Baillie, A. W. Y. Solar cell efficiency tables (version 54). Progress in Photovoltaics: Research and Applications. 27(7) (2019) pp. 565–575. DOI:10.1002/pip.3171 .

[7] Shah, A. Thin-Film Silicon Solar Cells. McEvoy's Handbook of Photovoltaics. vol 11 (2018) pp. 235–307. DOI: 10.1016/b978-0-12-809921-6.00008-2.

[8] Barreau, N., Duche, D., Ruiz, C. M., Escoubas, L., Simon, J.-J., Le Rouzo, J., & Bermudez, V. Innovative approaches in thin-film photovoltaic cells. Optical Thin Films and Coatings. (2018) pp. 595–632. DOI:10.1016/b978-0-08-102073-9.00016-3 .

[9] Dharmadasa, I. M. Latest developments in CdTe, CuInGaSe2 and GaAs/AlGaAs thin film PV solar cells. Current Applied Physics. 9(2) (2009) pp. 2–6. DOI:10.1016/j.cap.2008.12.021.

[10] Witte, W., Hariskos, D., Eicke, A., Menner, R., Kiowski, O., & Powalla, M. Impact of annealing on Cu(In,Ga)Se2 solar cells with Zn(O,S)/(Zn,Mg)O buffers. Thin Solid Films. 535 (2013) pp. 180–183. DOI:10.1016/j.tsf.2012.10.038 .

[11] J. Li et al., "Effects of substrate orientation and solution movement in chemical bath deposition on Zn(O,S) buffer layer and Cu(In,Ga)Se2 thin film solar cells," Nano Energy, 58 (2019) pp. 427–436. DOI: 10.1016/j.nanoen.2019.01.054.

[12] R. Klenk et al.Sputtered Zn(O,S): a promising approach to dry inline fabrication of Cdfree CIGS modules. 2014 IEEE 40th Photovoltaic Specialist Conference (PVSC). (2014) pp. 0959–0963. DOI: 10.1109/PVSC.2014.6925072.

[13] R. Klenk et al. Junction formation by Zn(O,S) sputtering yields CIGSe-based cells with efficiencies exceeding 18%. Progress in Photovoltaics: Research and Applications. vol. 22(2) (2014) pp. 161–165. DOI: 10.1002/pip.2445.

[14] G.-R. Uhm, S. Y. Jang, Y. H. Jeon, H. K. Yoon, and H. Seo. Optimized electronic structure of a Cu(In,Ga)Se 2 solar cell with atomic layer deposited Zn(O,S) buffer layer for high power conversion efficiency. RSC Advances. vol. 4 (53) (2014) pp. 28111–28118. DOI: 10.1039/c4ra01997k.

[15] Hildebrandt, T., Loones, N., Bouttemy, M., Vigneron, J., Etcheberry, A., Lincot, D., & Naghavi, N. Toward a Better Understanding of the Use of Additives in Zn(S,O) Deposition Bath for High-Efficiency Cu(In,Ga)Se2-Based Solar Cells. IEEE Journal of Photovoltaics. 5(6) (2015) 1821–1826. DOI:10.1109/jphotov.2015.2478066 .

[16] Johnson, R. W., Hultqvist, A., & Bent, S. F. A brief review of atomic layer deposition: from fundamentals to applications. Materials Today. 17(5) (2014) pp. 236–246. DOI:10.1016/j.mattod.2014.04.026.

[17] Yoo, Y.-Z., Jin, Z.-W., Chikyow, T., Fukumura, T., Kawasaki, M., & Koinuma, H. S doping in ZnO film by supplying ZnS species with pulsed-laser-deposition method. Applied Physics Letters. 81(20) (2002) pp. 3798–3800. DOI:10.1063/1.1521577

[18] Thankachan, R. M., & Balakrishnan, R. Synthesis Strategies of Single-Phase and Composite Multiferroic Nanostructures. Synthesis of Inorganic

Nanomaterials. (2018) pp. 185–211. DOI:10.1016/b978-0-08-101975-7.00008-7.

[19] Chopra, K. L., Paulson, P. D., & Dutta, V. Thin-film solar cells: an overview. Progress in Photovoltaics: Research and Applications. 12 (2004) pp. 69-92. DOI: 10.1002/pip.541 .

[20] T. Kirchartz, D. Abou-Ras & U. Rau. Introduction to Thin-Film Photovoltaics. In Advanced Characterization Techniques for Thin Film Solar Cells. Wiley-VCH Verlag GmbH & Co. KGaA (2011) pp. 1-32. DOI: 10.1002/9783527636280.ch1 .

[21] Philipps, S. P., Dimroth, F., & Bett, A. W. High-Efficiency III–V Multijunction Solar Cells. McEvoy's Handbook of Photovoltaics. (2018) pp. 439–472. DOI:10.1016/b978-0-12-809921-6.00012-4.

[22] Bao, Z., Liu, L., Yang, X., Tang, P., Yang, K., Lu, H., … Li, B. Synthesis and characterization of novel oxygenated CdSe window layer for CdTe thin film solar cells. Materials Science in Semiconductor Processing. 63 (2017) pp. 12-17. DOI: 10.1016/j.mssp.2017.01.003.

[23] G.Gordillo,M. Grizalez, L. Moreno & F. Landazábal. Influence of the Optical Window on the Performance of TCO/CdS/CdTe Solar Cells. Physica Status Solidi(b). 220 (2000) pp. 215-219. DOI: 10.1002/1521-3951(200007)220:1<215::AID-PSSB215>3.0.CO;2-8 .

[24] J. Deckers, E. Bourgeois, M. Jivanescu, A. Abass, D. Van Gestel, K. Van Nieuwenhuysen, B. Douhard, J. D'Haen, M. Nesladek, J. Manca, I. Gordon, H. Bender, A. Stesmans, R. Mertens, J. Poortmans, Comparing n- and p-type polycrystalline silicon absorbers in thin-film solar cells, Thin Solid Films. 579 (2015) pp. 144-152. DOI: 10.1016/j.tsf.2015.02.058.

[25] V. Krishnakumar, S. Barati, K. Jaegermann. A possible way to reduce absorber layer thickness in thin film CdTe solar cells. Thin Solid Films. 535 (2013) pp. 233-236. DOI: 10.1016/j.tsf.2012.11.085.

[26] Spiering, S., Eicke, A., Hariskos, D., Powalla, M., Naghavi, N., & Lincot, D. Large-area Cd-free CIGS solar modules with In2S3 buffer layer deposited by

ALCVD. In Thin Solid Films. 451 (2004) pp. 562-566. DOI: 10.1016/j.tsf.2003.10.090.

[27] D. Hariskos, S. Spiering, & M. Powalla . Buffer layers in Cu(In,Ga)Se_2 solar cells and modules. Thin Solid Films. 480 (2005) pp. 99-109. DOI: 10.1016/j.tsf.2004.11.118.

[28] Kato, T., Wu, J.-L., Hirai, Y., Sugimoto, H., & Bermudez, V. Record Efficiency for Thin-Film Polycrystalline Solar Cells Up to 22.9% Achieved by Cs-Treated Cu(In,Ga)(Se,S)2. IEEE Journal of Photovoltaics. (2018) pp. 1–6. DOI:10.1109/jphotov.2018.2882206 .

[29] Jackson, P., Wuerz, R., Hariskos, D., Lotter, E., Witte, W., & Powalla, M. Effects of heavy alkali elements in Cu(In,Ga)Se2 solar cells with efficiencies up to 22.6%. Physica Status Solidi (RRL) - Rapid Research Letters. 10(8) (2016) pp. 583–586. DOI:10.1002/pssr.201600199 .

[30] K.M. Hynes, J. Newham. Proceedings 16th European Photovoltaic Solar Energy Conference, Glasgow, UK. Vol. 2 (2000) 2297.

[31] Abhijit Kar. Nanoelectronics and Materials Developments. IntechOpen. 8 (2016). DOI: 10.5772/61560.

[32] Leoncini, M., Artegiani, E., Barbato, M., Meneghini, M., Meneghesso, G., Cavallini, M., & Romeo, A. Efficiency Improvement of CdTe Solar Cells with Ultra-Thin CdS Layer. 35th European Photovoltaic Solar Energy Conference and Exhibition. 11 (2018) pp. 889 - 891. DOI: 10.4229/35thEUPVSEC20182018-3BV.2.25 .

[33] Directive 2002/96/EC of the European parliament and of the council of 27 January 2003 on waste electrical and electronic equipment (WEEE), Official Journal of the European Union (2003) L37/24.

[34] Naghavi, Abou-Ras, Allsop, Barreau, Bücheler, Ennaoui, . . . Contreras, Miguel. Buffer layers and transparent conducting oxides for chalcopyrite Cu(In,Ga)(S,Se) 2 based thin film photovoltaics: Present status and current developments. Progress in Photovoltaics: Research and Applications. 18(6) (2010) pp. 411-433. DOI: 10.1002/pip.955.

[35] Friedlmeier, T. M., Jackson, P., Bauer, A., Hariskos, D., Kiowski, O., Wuerz, R., & Powalla, M. Improved Photocurrent in Cu(In,Ga)Se2 Solar Cells: From 20.8% to 21.7% Efficiency with CdS Buffer and 21.0% Cd-Free. IEEE Journal of Photovoltaics. 5(5) (2015) pp. 1487–1491. DOI: 10.1109/jphotov.2015.2458039.

[36] Perrenoud, J., Buecheler, S., Kranz, L., Fella, C., Skarp, J., & Tiwari, A. N. Application of ZnO1−xSx as window layer in cadmium telluride solar cells. 2010 35th IEEE Photovoltaic Specialists Conference. (2010) pp. 995-1000. DOI: 10.1109/pvsc.2010.5614592.

[37] Ericson, T., Scragg, J. J., Hultqvist, A., Watjen, J. T., Szaniawski, P., Torndahl, T., & Platzer-Bjorkman, C. Zn(O, S) Buffer Layers and Thickness Variations of CdS Buffer for Cu2ZnSnS4 Solar Cells. IEEE Journal of Photovoltaics, 4(1) (2014) pp. 465–469. DOI:10.1109/jphotov.2013.2283058.

[38] Nakamura, M., Yamaguchi, K., Kimoto, Y., Yasaki, Y., Kato, T., & Sugimoto, H. Cd-Free Cu(In,Ga)(Se,S)2 Thin-Film Solar Cell With Record Efficiency of 23.35%. IEEE Journal of Photovoltaics. 11 (2019) pp. 1–5. DOI: 10.1109/jphotov.2019.2937218.

[39] Kobayashi, T., Kao, Z. J. L., & Nakada, T. Temperature dependent current–voltage and admittance spectroscopy on heat-light soaking effects of Cu(In,Ga)Se2 solar cells with ALD-Zn(O,S) and CBD-ZnS(O,OH) buffer layers. Solar Energy Materials and Solar Cells. 143 (2015) pp. 159–167. DOI:10.1016/j.solmat.2015.06.044 .

[40] Sáez-Araoz, R., Krammer, J., Harndt, S., Koehler, T., Krueger, M., Pistor, P., … Fischer, C.-H. ILGAR In2S3buffer layers for Cd-free Cu(In,Ga)(S,Se)2 solar cells with certified efficiencies above 16%. Progress in Photovoltaics: Research and Applications. 20(7) (2012) 855–861. DOI:10.1002/pip.2268 .

[41] Lindahl, J., Zimmermann, U., Szaniawski, P., Torndahl, T., Hultqvist, A., Salome, P., … Edoff, M. Inline Cu(In,Ga)Se2 Co-evaporation for High-Efficiency Solar Cells and Modules. IEEE Journal of Photovoltaics. 3(3) (2013) pp. 1100–1105. DOI:10.1109/jphotov.2013.2256232.

[42] Cui, X., Sun, K., Huang, J., Lee, C.-Y., Yan, C., Sun, H., … Hao, X. Enhanced heterojunction interface quality to achieve 9.3% efficient Cd-free Cu2ZnSnS4 solar cells using ALD ZnSnO buffer layer. Chemistry of Materials.30(21) (2018) pp. 7860-7871. DOI: 10.1021/acs.chemmater.8b03398.

[43] Hejin Park, H., Heasley, R., & Gordon, R. G. Atomic layer deposition of Zn(O,S) thin films with tunable electrical properties by oxygen annealing. Applied Physics Letters. 102(13) (2013) pp. 132110.DOI:10.1063/1.4800928.

[44] Khomyak, V., Shtepliuk, I., Khranovskyy, V., & Yakimova, R. Band-gap engineering of ZnO1-xSx films grown by rf magnetron sputtering of ZnS target. Vacuum. 121 (2015) pp. 120–124. DOI: 10.1016/j.vacuum.2015.08.008.

[45] Jiang, J., Xu, H., Zhu, L., Niu, W., Guo, Y., Li, Y., Hu, L., He, H., & Ye, Z. Structural and optical properties of ZnSO alloy thin films with different S contents grown by pulsed laser deposition. Journal of Alloys and Compounds. 582 (2014) pp. 535–539. DOI: 10.1016/j.jallcom.2013.07.015.

[46] Barkhouse, D. A. R., Haight, R., Sakai, N., Hiroi, H., Sugimoto, H., & Mitzi, D. B. Cd-free buffer layer materials on Cu2ZnSn(SxSe1−x)4: Band alignments with ZnO, ZnS, and In2S3. Applied Physics Letters, 100(19) (2012) 193904. DOI:10.1063/1.4714737.

[47] Grimm, A., Kieven, D., Lauermann, I., Lux-Steiner, M. C., Hergert, F., Schwieger, R., & Klenk, R. Zn(O, S) layers for chalcoyprite solar cells sputtered from a single target. EPJ Photovoltaics. 3 (2012) pp. 30302. DOI:10.1051/EPJPV/2012011.

[48] Ericson, T., Scragg, J. J., Hultqvist, A., Watjen, J. T., Szaniawski, P., Torndahl, T., & Platzer-Bjorkman, C. Zn(O, S) Buffer layers and thickness variations of CDS buffer for Cu2ZnSnS4 solar cells. IEEE Journal of Photovoltaics. 4(1) (2014) pp. 465–469. DOI: 10.1109/JPHOTOV.2013.2283058.

[49] Hong, H. K., Kim, I. Y., Park, H. K., Jo, J., Song, G. Y., Kim, J. H., & Heo, J. Zn(O,S) buffer layers grown by atomic layer deposition in Cu2ZnSn(S,Se)4 thin film solar cells. Proceedings of AM-FPD 2015 - 22nd International Workshop on Active-Matrix Flatpanel Displays and Devices: TFT Technologies

and FPD Materials. (2015) pp. 199–201. DOI: 10.1109/AM-FPD.2015.7173241.

[50] Choi, W. J., Park, W. W., Kim, Y., Son, C. S., & Hwang, D. The effect of AlD-Zn(O,S) buffer layer on the performance of CIGSSe thin film solar cells. Energies. 13(2) (2020) 412 . DOI: 10.3390/en13020412.

[51] Sinsermsuksakul, P., Hartman, K., Bok Kim, S., Heo, J., Sun, L., Hejin Park, H., … Gordon, R. G. Enhancing the efficiency of SnS solar cells via band-offset engineering with a zinc oxysulfide buffer layer. Applied Physics Letters. 102(5) (2013) 053901. DOI:10.1063/1.4789855.

[52] Bugot, C., Broussillou, C., Sorba, A., Parissi, L., Schneider, N., Lincot, D., & Donsanti, F. Temperature effect during atomic layer deposition of zinc oxysulfide -Zn(O,S) buffer layers on Cu(In,Ga)(S,Se)2 synthesized by co-evaporation and electro-deposition techniques. 2015 IEEE 42nd Photovoltaic Specialist Conference (PVSC). 12 (2015) pp. 1-6. DOI: 10.1109/pvsc.2015.7356413.

[53] Bugot, C., Schneider, N., Jubault, M., Lincot, D., & Donsanti, F. Temperature effect on zinc oxysulfide-Zn(O,S) films synthesized by atomic layer deposition for Cu(In,Ga)Se2 solar cells. Journal of Vacuum Science & Technology A: Vacuum, Surfaces, and Films. 33(1) (2015) 01A151. DOI: 10.1116/1.4903366.

[54] Khemiri, N., Aousgi, F., & Kanzari, M. Tunable optical and structural properties of Zn(S,O) thin films as Cd-free buffer layer in solar cells. Materials Letters, 199 (2017) pp. 1–4. DOI: 10.1016/j.matlet.2017.04.037.

[55] Jani, M., Raval, D., Pati, R. K., Mukhopadhyay, I., & Ray, A. Effect of annealing atmosphere on microstructure, optical and electronic properties of spray-pyrolysed In-doped Zn(O,S) thin films. Bulletin of Materials Science, 41(1) (2018) 22 . DOI:10.1007/s12034-017-1542-6 .

[56] Ebrahimiasl, S., Yunus, W. M. Z. W., Kassim, A., & Zainal, Z. Synthesis of Nanocrystalline SnOx (x = 1–2) Thin Film Using a Chemical Bath Deposition Method with Improved Deposition Time, Temperature and pH. Sensors. 11(10) (2011) pp. 9207–9216. DOI:10.3390/s111009207.

[57] Lokhande, C. D., Gondkar, P. M., Mane, R. S., Shinde, V. R., & Han, S.-H. CBD grown ZnO-based gas sensors and dye-sensitized solar cells. Journal of Alloys and Compound. 475(1) (2009) pp. 304–311. DOI: 10.1016/j.jallcom.2008.07.025.

[58] Pawar, S. M., Pawar, B. S., Kim, J. H., Joo, O.-S., & Lokhande, C. D. Recent status of chemical bath deposited metal chalcogenide and metal oxide thin films. Current Applied Physics, 11(2) (2011) pp. 117–161. DOI: 10.1016/j.cap.2010.07.007.

[59] Mohd Fudzi, L., Zainal, Z., Lim, H., Chang, S.-K., Holi, A., & Sarif@Mohd Ali, M. Effect of Temperature and Growth Time on Vertically Aligned ZnO Nanorods by Simplified Hydrothermal Technique for Photoelectrochemical Cells. Materials. 11(5) (2018) 704. DOI: 10.3390/ma11050704 .

[60] M. D. Tyona , R. U. Osuji, C. D. Lokhande, F. I. Ezema. Photovoltaic Properties of Aluminum Doped Zinc Oxide Electrodes Based on Variation of Aluminum Impurities in the Semiconductor. Journal of Materials Physics and Chemistry. 6(1) (2018) pp. 9-16. DOI: 10.12691/jmpc-6-1-2 .

[61] Shah, N. A., Rabeel, Z., Abbas, M., & Syed, W. A. Effects of CdCl2 Treatment on Physical Properties of CdTe/CdS Thin Film Solar Cell. Modern Technologies for Creating the Thin-Film Systems and Coatings. 3 (2017) pp. 382-407.DOI:10.5772/67191 .

[62] Sharbati, S., Keshmiri, S. H., McGoffin, J. T., & Geisthardt, R. (2014). Improvement of CIGS thin-film solar cell performance by optimization of Zn(O,S) buffer layer parameters. Applied Physics A. 118(4) (2014) pp. 1259–1265. DOI:10.1007/s00339-014-8825-1.

[63] Bär, M., Ennaoui, A., Klaer, J., Kropp, T., Sáez-Araoz, R., Lehmann, S., Grimm, A., Lauermann, I., Loreck, C., Sokoll, S., Schock, H. W., Fischer, C. H., Lux-Steiner, M. C., & Jung, C. Intermixing at the heterointerface between ZnS/Zn(S,O) bilayer buffer and CuInS2 thin film solar cell absorber. Journal of Applied Physics. 100(6) (2006) 064911. DOI: 10.1063/1.2345034.

[64] M. Buffière, S. Harel, L. Arzel, C. Deudon, N. Barreau, and J. Kessler. Fast chemical bath deposition of Zn(O,S) buffer layers for Cu(In,Ga)Se 2 solar cells.

Thin Solid Films. vol. 519(21), (2011) pp. 7575–7578. DOI: 10.1016/j.tsf.2011.01.104.

[65] E. Gautron et al. Microstructural characterization of chemical bath deposited and sputtered Zn(O,S) buffer layers. Thin Solid Films. vol. 535(1) (2013) pp. 175–179. DOI: 10.1016/j.tsf.2012.10.040.

[66] Herrero, J., Gutiérrez, M. T., Guillén, C., Doña, J. M., Martínez, M. A., Chaparro, A. M., & Bayón, R. Photovoltaic windows by chemical bath deposition. Thin Solid Films. 361 (2000) pp. 28–33. DOI: 10.1016/S0040-6090(99)00830-5.

[67] Kopp Alves, A., Bergmann, C. P., & Berutti, F. A. Spray Pyrolysis.Engineering Materials. (2013) pp. 23–30. DOI: 10.1007/978-3-642-41275-2_3 .

[68] Sumanth Kumar, D., Jai Kumar, B., & Mahesh, H. M. Quantum Nanostructures (QDs): An Overview. Synthesis of Inorganic Nanomaterials. (2018) pp. 59–88. DOI:10.1016/b978-0-08-101975-7.00003-8.

[69] Filipovic, L., Selberherr, S., Mutinati, G. C., Brunet, E., Steinhauer, S., Köck, A., … Schrank, F. Methods of simulating thin film deposition using spray pyrolysis techniques. Microelectronic Engineering, 117 (2014) pp. 57–66. DOI:10.1016/j.mee.2013.12.025 .

[70] Gavrilović, T. V., Jovanović, D. J., & Dramićanin, M. D. Synthesis of Multifunctional Inorganic Materials. Nanomaterials for Green Energy. (2018) pp. 55–81. DOI:10.1016/b978-0-12-813731-4.00002-3.

[71] Ashik, U. P. M., Kudo, S., & Hayashi, J. An Overview of Metal Oxide Nanostructures. Synthesis of Inorganic Nanomaterials. (2018) pp. 19–57. DOI: 10.1016/b978-0-08-101975-7.00002-6 .

[72] Polat, İ., Aksu, S., Altunbaş, M., & Bacaksız, E. The influence of diffusion temperature on the structural, optical, and magnetic properties of nickel-doped zinc oxysulfide thin films. Physica Status Solidi (A). 209(1) (2012) pp. 160–166. DOI: 10.1002/pssa.201127248.

[73] Bari RH, Khadayate RS, Patil SB, Bari AR, Jain GH, Patil LA, Kale B.B. Preparation, characterization and H2S sensing performance of sprayed

nanostructured SnO2 thin films. ISRN Nanotechnology. (2012) pp. 1–5. DOI: 10.5402/2012/734325.

[74] Puurunen RL. Surface chemistry of atomic layer deposition: a case study for the trimethylaluminum water process. J Appl Phys. 97 (2005) 121301. DOI: 10.1063/1.1940727.

[75] George SM. Atomic layer deposition: an overview. Chem Rev. 110 (2010) 11131. DOI: 10.1021/cr900056b.

[76] M. Godlewski, "Atomic layer deposition," Semiconductor Science and Technology. Vol. 27 (7) (2012) p. 1.

[77] Muneshwar, T., Miao, M., Borujeny, E. R., & Cadien, K. Atomic Layer Deposition: Fundamentals, Practice, and Challenges. In Handbook of Thin Film Deposition: Fourth Edition. Elsevier. (2018) pp. 359–377. DOI : 10.1016/B978-0-12-812311-9.00011-6.

[78] Alam, A. U., Qin, Y., Nambiar, S., Yeow, J. T. W., Howlader, M. M. R., Hu, N.-X., & Deen, M. J. Polymers and organic materials-based pH sensors for healthcare applications. Progress in Materials Science. 96 (2018) pp. 174–216. DOI:10.1016/j.pmatsci.2018.03.008.

[79] Larsson, F., Donzel-Gargand, O., Keller, J., Edoff, M., & Törndahl, T. Atomic layer deposition of Zn(O,S) buffer layers for Cu(In,Ga)Se2 solar cells with KF post-deposition treatment. Solar Energy Materials and Solar Cells. 183 (2018) pp. 8–15. DOI : 10.1016/j.solmat.2018.03.045.

[80] Lin, X., Li, H., Qu, F., Gu, H., & Wang, W. Cu(In,Ga)Se2 solar cell with Zn(S,O) as the buffer layer fabricated by a chemical bath deposition method. Solar Energy. 171(2018) pp. 130–141. DOI: 10.1016/j.solener.2018.06.070.

[81] Platzer-Björkman, C., Törndahl, T., Abou-Ras, D., Malmström, J., Kessler, J., & Stolt, L. Zn(O,S) buffer layers by atomic layer deposition in Cu(In,Ga)Se2 based thin film solar cells: Band alignment and sulfur gradient. Journal of Applied Physics. 100(4) (2006) 044506. DOI :10.1063/1.2222067.

[82] Simon, A. H. Sputter Processing. In Handbook of Thin Film Deposition: Fourth Edition. Elsevier. (2018) pp. 195–230. DOI: 10.1016/B978-0-12-812311-9.00007-4.

[83] Gudmundsson, J. T., & Lundin, D. Introduction to magnetron sputtering. In High Power Impulse Magnetron Sputtering: Fundamentals, Technologies, Challenges and Applications. Elsevier. 1 (2019) pp. 1–48. DOI: 10.1016/B978-0-12-812454-3.00006-1.

[84] Sarkar, J. Sputtering and Thin Film Deposition. In Sputtering Materials for VLSI and Thin Film Devices) . Elsevier. (2014) pp. 93–170. DOI: 10.1016/b978-0-8155-1593-7.00002-3.

[85] Depla, D., Mahieu, S., & Greene, J. E. Sputter Deposition Processes. In Handbook of Deposition Technologies for Films and Coatings . Elsevier Inc. (2010) pp. 253–296. DOI: 10.1016/B978-0-8155-2031-3.00005-3.

[86] Orava, J., Kohoutek, T., & Wagner, T. Deposition techniques for chalcogenide thin films. In Chalcogenide Glasses. Elsevier Ltd. (2013) pp. 265–309. DOI: 10.1533/9780857093561.1.265.

[87] Cho, D. H., Lee, W. J., Shin, B., & Chung, Y. D. Analysis of vertical phase distribution in reactively sputtered zinc oxysulfide thin films. Applied Surface Science. 486 (2019) pp. 555–560. DOI: 10.1016/j.apsusc.2019.04.200.

[88] Grimm, A., Kieven, D., Lauermann, I., Lux-Steiner, M. C., Hergert, F., Schwieger, R., & Klenk, R. Zn(O, S) layers for chalcoyprite solar cells sputtered from a single target. EPJ Photovoltaics. 3 (2012) 30302. DOI: 10.1051/epjpv/2012011.

[89] Zafar, M. S., Farooq, I., Awais, M., Najeeb, S., Khurshid, Z., & Zohaib, S. Bioactive Surface Coatings for Enhancing Osseointegration of Dental Implants. Biomedical, Therapeutic and Clinical Applications of Bioactive Glasses. (2019) pp. 313–329. DOI :10.1016/b978-0-08-102196-5.00011-2 .

[90] Grimm, A., Just, J., Kieven, D., Lauermann, I., Palm, J., Neisser, A., … Klenk, R. Sputtered Zn(O,S) for junction formation in chalcopyrite-based thin film solar cells. Physica Status Solidi (RRL) - Rapid Research Letters. 4(6) (2010) pp. 109–111. DOI:10.1002/pssr.201004083.

[91] Sarkar, J. Troubleshooting in Sputter Deposition. In Sputtering Materials for VLSI and Thin Film Devices. Elsevier. Vol. 1 (2014) pp. 567–592. DOI: 10.1016/b978-0-8155-1593-7.00008-4.

[92] L. R. Shaginyan . Pulsed laser deposition of thin films: Expectations and reality. (2002) pp. 627–673. DOI: 10.1016/B978-012512908-4/50016-3 .

[93] Fujioka, H. Pulsed Laser Deposition (PLD). In Handbook of Crystal Growth: Thin Films and Epitaxy: Second Edition. Elsevier Inc. Vol. 3 (2015) pp. 365–397. DOI: 10.1016/B978-0-444-63304-0.00008-1.

[94] Eason, R. W., May-Smith, T. C., Sloyan, K., Gazia, R., Darby, M., & Sposito, A. Emerging pulsed laser deposition techniques. Laser Growth and Processing of Photonic Devices. (2012) pp. 55–84. DOI: 10.1533/9780857096227.1.53 .

[95] Adachi, H., & Wasa, K. Thin Films and Nanomaterials. Handbook of Sputtering Technology. (2012) pp. 3–39. DOI: 10.1016/b978-1-4377-3483-6.00001-2 .

[96] Shah, S. I., Jaffari, G. H., Yassitepe, E., & Ali, B. Evaporation. Handbook of Deposition Technologies for Films and Coatings. (2010) pp. 135–252. DOI: 10.1016/b978-0-8155-2031-3.00004-1 .

[97] Sarangan, A. Nanofabrication. Fundamentals and Applications of Nanophotonics. (2016) pp. 149–184. DOI: 10.1016/b978-1-78242-464-2.00005-1.

[98] Halada, G. P., & Clayton, C. R. The Intersection of Design, Manufacturing, and Surface Engineering. Handbook of Environmental Degradation of Materials. (2012) pp. 443–480. DOI:10.1016/b978-1-4377-3455-3.00015-8 .

[99] Mittra, J., Abraham, G. J., Kesaria, M., Bahl, S., Gupta, A., Shivaprasad, S. M., … Dey, G. K. Role of Substrate Temperature in the Pulsed Laser Deposition of

Zirconium Oxide Thin Film. Materials Science Forum. 710 (2012) pp. 757–761. DOI: 10.4028/www.scientific.net/msf.710.757.

[100] Deulkar, S. H., Huang, J.-L., & Neumann-Spallart, M. Zinc Oxysulfide Thin Films Grown by Pulsed Laser Deposition. Journal of Electronic Materials. 39(5) (2010) pp. 589–594. DOI:10.1007/s11664-009-1069-8 .

[101] Bereznev, S., Kocharyan, H., Maticiuc, N., Naidu, R., Volobujeva, O., Tverjanovich, A., & Kois, J. One-stage pulsed laser deposition of conductive zinc oxysulfide layers. Applied Surface Science. 425 (2017) pp. 722–727. DOI: 10.1016/j.apsusc.2017.07.078.

[102] Cheng, Q., Wang, D., & Zhou, H. Electrodeposition of Zn(O,S) (zinc oxysulfide) thin films: Exploiting its thermodynamic and kinetic processes with incorporation of tartaric acid. Journal of Energy Chemistry. 27(3) (2018) pp. 913–922. DOI: 10.1016/j.jechem.2017.07.020.

[103] Zhang, J., Feng, J., Feng, Y., Liao, J., Xue, S., Shao, L., & Liang, G. Fabrication of Zn(O,S) thin films by ozone assisted photochemical deposition and its potential applications as buffer layers in kesterite-based thin film solar cells. Thin Solid Films. 670 (2018) pp.80-85. DOI:10.1016/j.tsf.2018.12.002

[104] Kriisa, M., Sáez-Araoz, R., Fischer, C.-H., Köhler, T., Kärber, E., Fu, Y., … Krunks, M. Study of Zn(O,S) films grown by aerosol assisted chemical vapour deposition and their application as buffer layers in Cu(In,Ga)(S,Se)2 solar cells. Solar Energy. 115 (2015) pp. 562–568. DOI: 10.1016/j.solener.2015.02.046.

[105] Hong, R., Shao, J., He, H., & Fan, Z. Influence of buffer layer thickness on the structure and optical properties of ZnO thin films. Applied Surface Science. 252(8) (2006) pp. 2888–2893. DOI:10.1016/j.apsusc.2005.04.041

[106] Sun, J., Nalla, V., Nguyen, M., Ren, Y., Chiam, S. Y., Wang, Y., … Wong, L. H. Effect of Zn(O,S) buffer layer thickness on charge carrier relaxation dynamics of CuInSe 2 solar cell. Solar Energy. 115 (2015) pp. 396–404. DOI:10.1016/j.solener.2015.03.008

[107] Bär, M., Ennaoui, A., Klaer, J., Kropp, T., Sáez-Araoz, R., Allsop, N., … Lux-Steiner, M. C.. Formation of a ZnS/Zn(S,O) bilayer buffer on CuInS2 thin film solar cell absorbers by chemical bath deposition. Journal of Applied Physics. 99(12) (2006) 123503. DOI:10.1063/1.2202694

[108] Shi, S., He, Z., Fan, Y., Liu, Y., Zhang, Y., Cheng, S., … Liu, W. Optimizing the thickness of sputtering-Zn(O, S) buffer layer for all-dry Cd-free CIGS solar cells. Materials Research Express. 6(8) (2019) pp. 086431. DOI: 10.1088/2053-1591/ab200a.

[109] K. Ramanathan et al., "A comparative study of Zn(O,S) buffer layers and CIGS solar cells fabricated by CBD, ALD, and sputtering," 2012 38th IEEE Photovoltaic Specialists Conference, Austin, TX. (2012) pp. 001677-001681. DOI: 10.1109/PVSC.2012.6317918.

[110] Richard R. Zito "Ion-air gun cleaning of substrates prior to thin film deposition", Proc. Advances in Thin-Film Coatings for Optical Applications II. Vol. 5870(1) (2005) 587005. DOI: 10.1117/12.612877.

[111] Kohli, R. Applications of UV-Ozone Cleaning Technique for Removal of Surface Contaminants. Developments in Surface Contamination and Cleaning: Applications of Cleaning Techniques. (2019) pp. 355–390. DOI:10.1016/b978-0-12-815577-6.00009-8

[112] Cullity, B. D., & Stock, S. R. Elements of X-ray Diffraction, Third Edition. Upper Saddle River, N.J.: Prentice-Hall. (2001).

[113] A. Yoshida, Y. Kaburagi, and Y. Hishiyama. Chapter 5 - Scanning Electron Microscopy. Materials Science and Engineering of Carbon: Characterization. Elsevier Inc. (2016) pp. 71–93. DOI: 10.1016/B978-0-12-805256-3.00005-2.

[114] Abd Mutalib, M., Rahman, M. A., Othman, M. H. D., Ismail, A. F., & Jaafar, J. Scanning Electron Microscopy (SEM) and Energy-Dispersive X-Ray (EDX) Spectroscopy. Membrane Characterization. (2017) pp. 161–179. DOI:10.1016/b978-0-444-63776-5.00009-7.

[115] Karoui, R. Spectroscopic Technique: Fluorescence and Ultraviolet-Visible (UV-Vis) Spectroscopies. Modern Techniques for Food Authentication. (2018) pp. 219–252. DOI:10.1016/b978-0-12-814264-6.00007-4.

[116] Mir, F. A., Bhat, G. M., Asokan, K., Batoo, K. M., & Banday, J. A. Crystal structure, morphological, optical and electrical investigations of Oxypeucedanin micro crystals: an isolated compound from a plant. Journal of Materials Science: Materials in Electronics. 25(1) (2013) pp. 431–437. DOI:10.1007/s10854-013-1606-3

[117] Pütz, J., Heusing, S., & Aegerter, M. A. Characterization of Electrical Properties. Handbook of Sol-Gel Science and Technology. (2016) pp. 1–30. DOI:10.1007/978-3-319-19454-7_52-1.

[118] Vani, V. P. Geetha, Reddy, M. Vasudeva, & Reddy, K. T. Ramakrishna. (2013). Thickness-Dependent Physical Properties of Coevaporated CuSnS Films. ISRN Condensed Matter Physics. 10 (2013) pp. 1-6. DOI:10.1155/2013/142029.

[119] Mridha, S., & Basak, D. Effect of thickness on the structural, electrical and optical properties of ZnO films. Materials Research Bulletin. 42(5) (2007) pp. 875–882. DOI: 10.1016/j.materresbull.2006.08.019 .

[120] Bouguila, N., Kraini, M., Halidou, I., Lacaze, E., Bouchriha, H., & Bouzouita, H. Thickness Effect on Properties of Sprayed In2S3 Films for Photovoltaic Applications. Journal of Electronic Materials. 45(1) (2015) pp. 829–838. DOI:10.1007/s11664-015-4216-4 .

[121] Sihan Shi, Zhichao He, Yu Fan, Yang Liu, Yunxiang Zhang, Shiqing Cheng, Shu Xu, Yi Zhang, Fangfang Liu, Zhiqiang Zhou, Andong Tang, Yun Sun and Wei Liu. Optimizing the thickness of sputtering-Zn(O,S) buffer layer for all-dry Cd-free CIGS solar cells. Materials Research Express. IOP Publishing. Vol 6 (2019) pp. 2053-1591. DOI: 10.1088/2053-1591/ab200a .

[122] M. Bouderbala, S. Hamzaoui, B. Amrani, A. H. Reshak, M. Adnane, T. Sahraoui, and M. Zerdali. Phys. Rev. B: Condens. Matter. 403 (2008) pp. 3326. DOI: 10.1016/j.physb.2008.04.045.

[123] Kumar, V., Singh, S. K., Sharma, H., Kumar, S., Banerjee, M. K., & Vij, A. Investigation of structural and optical properties of ZnO thin films of different thickness grown by pulse laser deposition method. Physica B: Condensed Matter. 552 (2018) pp. 221-226. DOI:10.1016/j.physb.2018.10.004 .